#432

LA-10335-MS

Los Alamos National Laboratory is operated by the University of California for the United States Department of Energy under contract W-7405-ENG-36.

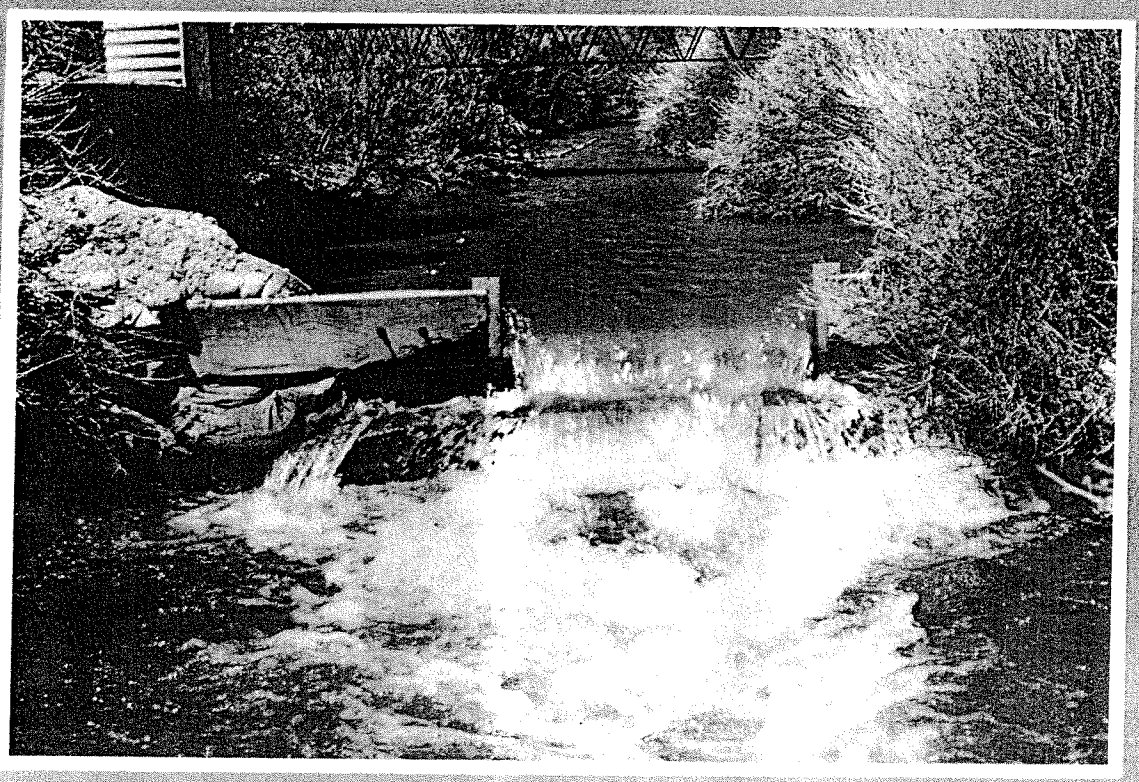

New Estimating Procedures for Surface Runoff, Sediment Yield, and Contaminant Transport in Los Alamos County, New Mexico

Los Alamos
Los Alamos National Laboratory
Los Alamos, New Mexico 87545

LA-10335-MS

UC-11
Issued: April 1985

New Estimating Procedures for Surface Runoff, Sediment Yield, and Contaminant Transport in Los Alamos County, New Mexico

Leonard J. Lane*
William D. Purtymun
Naomi M. Becker

*USDA-ARS Southwest Rangeland Watershed Research Center, 2000 E. Allen Road, Tucson, AZ 85719.

Los Alamos National Laboratory
Los Alamos, New Mexico 87545

Cover photo: Snowmelt runoff through a gaging station in the midreach of Los Alamos Canyon.

Photocomposition by Kathy Derouin, Group HSE-8

CONTENTS

TABLES

FIGURES

NEW ESTIMATING PROCEDURES FOR SURFACE RUNOFF, SEDIMENT YIELD, AND CONTAMINANT TRANSPORT IN LOS ALAMOS COUNTY, NEW MEXICO

by

Leonard J. Lane, William D. Purtymun, and Naomi M. Becker

ABSTRACT

Procedures are developed to predict runoff, sediment yield, and contaminant transport from semiarid watersheds with alluvial stream channels. The procedures represent a synthesis of mathematical models to approximate the complex processes of runoff generation, streamflow-routing and hydrograph development, sediment transport and yield, particle sorting and enrichment, and transport of sediment-associated contaminants.

The procedures are applied to a complex watershed-channel system at Los Alamos, New Mexico, and are used to compute plutonium transport and redistribution in alluvial stream channels. Mass-balance calculations are used to compute the amount of plutonium discharge from the channel system and to compute the plutonium remaining in storage in the channel alluvium.

I. INTRODUCTION

The term "watershed" means an area above a specified point on a stream channel enclosed by a perimeter. The watershed perimeter defines an area where surface runoff will move into the stream or its tributaries above the specified point. In arid and semiarid regions, where the surface features are most evident, a striking feature of the landscape is the stream channels, and thus watersheds, combining in complex patterns to produce the channel networks and interchannel areas. These features, in turn, control the routes and rates of movement of water and sediment, when precipitation causes runoff.

Because the entire surface of the land is composed of watersheds, and because hydrologic processes are complex and highly variable in time and space, hydrologic processes are impossible to measure on every watershed where information is needed. Moreover, because the hydrologic processes are influenced by variable climate, geology and geologic materials, soils, vegetation, and land use, monitoring a few watersheds and extending the results over large areas may give inaccurate conclusions. Therefore, mathematical models are needed to mimic or simulate hydrologic processes on watersheds representing a wide variety of climate, soils, topography, and land use. This report describes the development and application of procedures to simulate hydrologic, hydraulic, and sedimentation processes on semiarid watersheds, and applies the procedures in computing contaminant transport rates.

A. Objectives

The first objective is to develop a hydrologic model or component to simulate the rates and amounts of runoff occurring on semiarid watersheds and to develop procedures for estimating model

parameters from physical features of the watershed and from established relationships.

The second objective is to simulate open-channel flow hydraulics and the resulting sediment transport rates and sediment yield. This objective includes estimating model parameters from physical features of the channel system and from established relationships.

The third objective is to combine the hydrologic and sediment components to predict rates and amounts of runoff and sediment yield from semiarid watersheds.

The fourth objective is to develop procedures for using the simulation models to study the movement of runoff and sediment-associated contaminants in complex semiarid watersheds.

Collectively, these objectives represent an attempt to develop reasonably simple, yet physically based, simulation models for predicting runoff, sediment yield, and contaminant transport on semiarid watersheds.

B. Scope, Limitations, and Emphasis

The models described here apply to small semiarid watersheds with well-defined channel systems where the streamflow is ephemeral or intermittent. Because the sediment yield calculations are based on computed transport capacity, the procedures are designed to compute sediment transport capacity in alluvial stream channels composed of noncohesive sediments. Contaminant transport calculations are based on the assumption that the contaminants are adsorbed or strongly associated with the sediment particles. Finally, because many of the basic relationships incorporated in the model were developed using data from semiarid rangelands in the western United States, streamflow occurring in ephemeral channels as a result of rainfall events is emphasized.

C. Brief Overview

The procedure for computation of runoff, sediment, and contaminant transport is summarized in Fig. 1. Based on climatic inputs, watershed characteristics, and land use, the hydrologic component estimates runoff delivery to the channel system from the upland and lateral flow areas. The streamflow routing procedure estimates runoff volume, peak runoff rate, and flow duration at any position in the channel system. Runoff data provide input to the sediment yield component. Hydraulic calculations are made for velocity, flow depth, hydraulic radius, and shear stress for nine discrete time intervals during flow in the channel. Transport capacity is computed for up to 10 sediment particle size classes, including suspended and bed load. Sediment transport rates are integrated over the nine time intervals approximating the hydrograph to estimate sediment yield at any point in the channel system. Sediment data are used in differential or difference equations for contaminant transport to

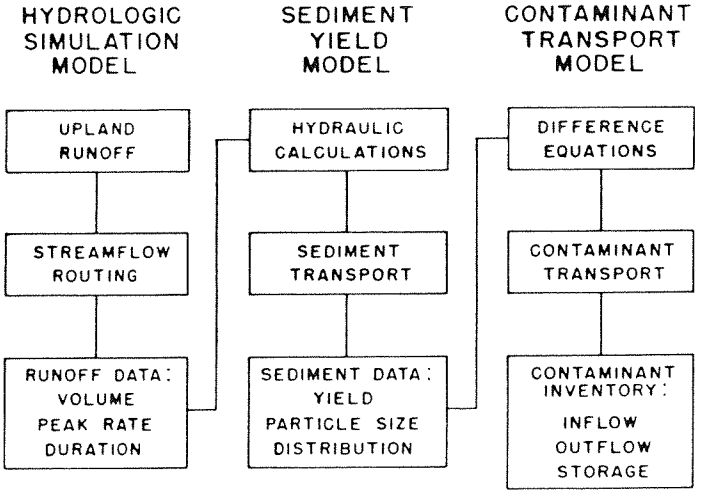

Fig. 1. Logic diagram for computation of runoff, sediment, and contaminant transport in semiarid water sheds.

estimate a contaminant inventory for each channel segment in the channel network.

This model features the capabilities of varying rainfall inputs over the upland and lateral flow areas through the entire watershed and the ability of the streamflow routing procedure to incorporate reductions in runoff volume and peak rate resulting from transmission losses in the channel alluvium. The hydraulic component simulates spatially varied and unsteady flow through the piecewise normal hydrograph technique. Runoff volume, peak rate, and flow duration are changed, and thus the hydrograph is changed in the downstream direction. Spatial variability owing to changes in channel geometry, transmission losses, and lateral inflow are approximated. Changing the flow rate, depth, velocity, and shear stress for each time interval on the hydrograph can approximate unsteady flow at a channel cross section. Assuming uniform and steady, or normal, flow during each nine time intervals on the hydrograph allows application of both the Manning equation to compute flow variables and sediment transport equations based on the normal flow assumption.

Sediment transport calculations are based on the particle size distribution of the channel bed sediments with different equations for suspended and bed-load sediment transport. Total sediment yield for a storm is estimated by integrating the transport rates throughout the hydrograph. Particle size distributions of the transported sediment are compared with the corresponding channel alluvium distributions to simulate the processes of particle sorting and enrichment of the transported sediment in the fines, or smaller sized sediments.

The enrichment computed from particle sorting information and the contaminant concentration particle size relationships are used to estimate transported contaminant concentrations relative to the mean contaminant concentration in the channel alluvium. These data are used in difference equations to compute a contaminant inventory in each channel segment and in the entire channel network.

D. Background

Background material on hydrologic, sediment, and contaminant transport processes on semiarid watersheds is summarized in Table I. The references in the table provide a technical overview and sources for many of the data upon which the procedures described herein are based.

II. DEVELOPMENT OF THE HYDROLOGIC COMPONENT

The hydrologic component consists of procedures to (1) estimate runoff from upland and lateral flow areas, (2) route streamflow in alluvial channels, (3) approximate the shape of runoff hydrographs, and (4) combine these processes into a distributed hydrologic simulation model.

A. Runoff from Upland Areas

The term "upland runoff" denotes runoff delivered upstream in a channel segment and also denotes runoff from lateral flow areas delivered along the length of a channel reach.

B. Infiltration and Runoff Volume

The Soil Conservation Service (SCS) method is widely used to calculate direct runoff from rainfall. Because of this method's widespread acceptance, existing parameter estimates and estimation techniques, and because its design incorporates changes in watershed conditions and land use, we adopted it as a procedure to estimate upland runoff volumes. The SCS runoff equation (NEH-4, 1972) is

$$V = \begin{cases} 0 \\ \dfrac{(P - 0.2S)^2}{(P + 0.8S)} \end{cases} \qquad (1)$$

where

V = runoff volume in in. (mm),
P = storm rainfall depth in in. (mm), and
S = retention parameter in in. (mm).

The parameter S in Eq. (1) is related to a runoff curve number CN so that

$$CN = \frac{1000}{10 + S} \qquad (2)$$

in English units and

$$CN = \frac{25\,400}{254 + S} \qquad (3)$$

Table I. Selected References for Hydrologic, Sediment, and Contaminant Transport Processes on Semiarid Watersheds

Process or Component	Comments	References
Hydrology of semiarid rangelands	Basic source material: technical overview	Branson et al. 1981 Renard, 1970
Upland runoff:	SCS[a] runoff equation	NEH-4, 1972
Infiltration	Influence of basin characteristics	Murphey et al. 1977
Hydrographs	Shape	Diskin and Lane 1976
Stream routing:		
Transmission losses	Routing equations	Lane 1980
Hydraulics	Basic equations	Chow 1959
Sediment transport:		
Equations	Basic source material	Graf 1971
Model	Procedure development	Lane 1982b
Contaminant transport:		
Transport	General overview	Watters et al. 1982 Knisel 1980
Model	Procedure development	Lane and Hakonson 1982

[a]US Department of Agriculture, Soil Conservation Service.

in metric units. Values of curve number vary from 0 (no runoff) to 100 (all rainfall becomes runoff).

When we apply Eq. (1) to upland or lateral flow area, curve number can represent a homogeneous area; an average or composite value for the area; or an area subdivided into subareas, each with its own curve number. Variations in curve number reflect soil type and structure, vegetation and cover management, and antecedent soil moisture.

C. Estimating Runoff Curve Numbers

The basic source material for estimating curve numbers is the SCS National Engineering Handbook (NEH-4 1972). However, additional research to determine curve numbers, especially under semiarid conditions, has been reported. This section summarizes curve numbers from the SCS Handbook and from other sources for antecedent soil moisture condition II (average or normal); descriptive variables are listed in the original English units.

Hydrologic soil groups and their general characteristics are summarized in Table II. Given the hydrologic soil group, curve numbers for various cover types, densities, and conditions are listed in Table III. Table IV lists curve numbers for various surface types ranging from unimproved bare soil to surfaces that are nearly impervious. Table V shows the per cent of impervious cover for various degrees of urbanization, and it shows how the per cent of impervious cover is used to derive a composite curve number to reflect urbanization influence. The SCS National Engineering Handbook describes procedures incorporating the influence of antecedent moisture on curve numbers. However, most practical applications usually involve the assumption of antecedent moisture condition II during the surface runoff simulation.

Table II. Soils Descriptions and Hydrologic Soil Groups (NEH-4, 1972)

Soil Group	Characteristics	Comments
A	Soils with high infiltration rates, even when wetted; well- to very well drained gravel, sand, loamy sands, and sandy loam; soils of 36 in. or deeper without infiltration-reducing layers	Low runoff potential and low CN
B	Soils with moderate infiltration rates; moderately well to well-drained soils with moderately fine to moderately coarse texture, usually moderately deep soils (20 in. or deeper)	Low to moderate runoff potential and CNs
C	Soils with slow infiltration rates; soils with moderately fine to fine texture, or with an infiltration-reducing layer; usually less than 20 in. of soil over an infiltration-impeding layer	Moderate to high runoff potential and CNs
D	Soils with very slow infiltration rates; clay soils with swelling potential, shallow soils over a clay layer, and shallow soils over nearly impervious material; usually less than 12 in. of soil over an infiltration-restricting layer	High runoff potential and high CNs

D. Streamflow Routing

Although the procedures described herein were derived for ephemeral stream channels with transmission losses, they can be applied, with somewhat coarser approximations, in alluvial channels without significant transmission losses.

E. Transmission Losses

Many semiarid watersheds have broad alluvium-filled channels that abstract large quantities of streamflow (Babcock and Cushing 1941; Burkham 1970a, 1970b; Renard 1970). These abstractions, or transmission losses, are important because water is lost as the flood wave travels downstream, and thus runoff volumes are reduced. Although these abstractions are called transmission losses, they are an important part of the water balance, because they support riparian vegetation and they recharge local aquifers and regional ground water (Renard 1970).

Several procedures have been developed to estimate transmission losses. These procedures include inflow loss rate equations (Burkham 1970a, 1970b; NEH-4 1972), simple regression equations (Lane, Diskin, and Renard 1971), simplified differential equations for loss rate (Jordan 1977; Lane 1980), storage routing for a cascade of leaky reservoirs (Lane 1972, Wu 1972, Peebles 1975), and kinematic wave models incorporating infiltration (Smith 1972). Therefore, procedures range in complexity for estimating runoff in ephemeral streams with transmission losses. As a rule, the simplified procedures require less information about physical features of watersheds, but are more specific in their application. The more complex procedures may be more physically based, but they require

Table III. Hydrologic Soil-Cover Complexes and Associated CNs
(NEH-4 1972; Zeller 1979; Branson et al. 1981)

Cover Type, Density, or Condition	CN (by hydrologic soil group)			
	A	B	C	D
Unimproved bare soil	72	82	87	90
Desert brush (% cover):				
<10	--	84	88	93
≃20	--	83	87	92
≃40	--	82	86	90
Pasture or range:				
Poor	68	79	86	89
Fair	49	69	79	84
Good	39	61	74	80
Herbaceous plants and grass (% cover):				
20	--	79	86	92
40	--	74	82	90
60	--	69	77	88
Piñon-juniper-grass (% cover):				
40	--	65	75	88
60	--	57	70	86
80	--	48	62	83
Ponderosa pine (% cover):				
40	--	61	75	80
60	--	55	70	77
80	--	49	65	73

Table IV. Approximate CNs for Bare Soil and Impervious Areas
(NEH-4 1972, Zeller 1979)

Surface Type	CNs (by hydrologic soil group)			
	A	B	C	D
Unimproved bare soil	72	82	87	90
Hard-surface dirt roads	74	84	90	92
Exposed bare rock	96	96	96	96
Completely impervious urban areas	99	99	99	99

Table V. Approximate Urbanization Influence upon Degree of Impervious Areas (Zeller 1979)

Development Type	% Impervious Cover[a] min	av	max
Suburban:			
<1 house per acre	5	10	20
≃1 house per acre	15	20	25
≃2 houses per acre	25	30	35
Light to moderate urbanization:			
≃3 houses per acre	30	35	40
≃4 houses per acre	35	40	45
≃5 houses per acre	45	50	55
Highly urbanized:			
Multiple dwellings	50	65	90
Light industry and commercial	50	70	80
Heavy industry and commercial	80	90	95+

[a]Composite curve number calculated as

$$CN = \frac{CN_0(100 - u) + 99u}{100} ,$$

where CN_0 is the curve number for natural conditions and u is the per cent impervious area.

correspondingly more data and more complex computations.

The simulation model presented herein attempts to develop a procedure for practical applications. The model is a compromise between the more physically based deterministic models and the more simplified procedures described in earlier references. The resulting model is constructed so as to require a minimum of observed data for calibration and to provide a means of predicting on ungaged watersheds.

Observations from many locations suggest that runoff from semiarid watersheds generally follows periods of thunderstorm rainfall, and at other times, the stream channels are normally dry. Runoff is accompanied by substantial infiltration losses in the stream channels. These losses, and the usually steep slope of the channels, tend to produce sharply peaked runoff hydrographs. The resulting shape of the hydrographs, which start from and end in conditions of no flow, consists of a fairly narrow triangular peak followed by a relatively longer recession of low flow. The time to peak (time from beginning of runoff to the hydrograph peak) is usually shorter than the recession time. This characteristic shape of the runoff hydrographs suggests that they can be fairly well approximated if the runoff volume, peak rate, time to peak, and duration of flow are known. Moreover, if the ratio of time to peak and duration is relatively constant, then the relation between runoff volume and peak rate is nearly linear. Based on these observations, the model described herein simulates a runoff volume and a flow duration, and then simulates peak flow

rate as a function of runoff volume and flow duration.

To route flow through the channel network, we must know peak discharge as well as runoff volume from the upland and lateral flow areas. Peak discharge is assumed to be a function of runoff volume and time characteristics of the runoff hydrograph. Peak discharge of a unit hydrograph from small areas can be estimated from runoff volume and time to peak (NEH-4 1972) as

$$Q = \frac{484VA}{T_p} \quad , \tag{4}$$

where, in English units, the variables are

Q = peak rate (in cfs),
V = runoff volume (in in.),
A = drainage area (in sq. mi.), and
T_p = time to peak (in h).

The conversion factor 484 converts units of square miles-inches per hour to cubic feet per second. If time to peak T_p is assumed to be a constant proportion of flow duration D, and discharge is expressed in inches per hour, then Eq. (4) becomes

$$Q = \frac{484\alpha V}{640D} \quad , \tag{5}$$

where

Q = peak discharge (in in./h),
α = the ratio of flow duration to peak time.
D = flow duration (in h),
$T_p = D/\alpha$, and

the conversion factor 640 is the number of acres per square mile. For a constant α, Eq. (5) is of the form

$$Q = C_5V/D \quad , \tag{6}$$

where C_5 is a parameter expressing hydrograph shape.

The use of a double-triangle unit hydrograph as a model for unit hydrographs of small watersheds has been proposed by Ardis (1972, 1973); with results for a number of watersheds published in a report by TVA 1973. These procedures were applied to a small semiarid watershed by Diskin and Lane (1976). Based on analysis of 10 hydrographs from a 4-acre (1.6-ha) watershed, they found that for a 1-min hydrograph,

$$u = 6.6V/\bar{D} \quad , \tag{7}$$

where u is the peak of the unit hydrograph, V is runoff volume in inches and $\bar{D}$ is the duration of the mean unit hydrograph in hours. By convoluting the unit hydrograph with observed excess rainfall patterns, the relation between runoff volume, mean flow duration, and peak runoff rate was

$$Q = 4.82V/\bar{D} \quad , \tag{8}$$

or $C_5 = 4.82$.

Using data from 15 semiarid watersheds in Arizona with 10 to 35 yr of record, Murphey et al. (1977) found that mean flow duration was related to drainage area as

$$\bar{D} = C_1A^{C2} = 2.53A^{0.2} \quad , \tag{9}$$

where

$\bar{D}$ = mean duration of flow (in h),
A = drainage area (in sq. mi.), and
C_1, C_2 = parameters.

The coefficient of determination for Eq. (9) was 0.78, with a standard error of 21%. They also found that mean runoff volume per runoff event was related to drainage area as

$$\bar{V} = C_3AC^4 = 0.05A^{-0.2} \quad , \tag{10}$$

where

$\bar{V}$ = mean runoff volume (in in.),
A = drainage area (in sq. mi), and
C_3, C_4 = parameters.

The coefficient of determination for Eq. (10) was 0.61, with a standard error of 28%.

A similar equation for mean peak discharge was found to be

$$\bar{Q} = 0.10A^{-0.38} \quad , \tag{11}$$

where

$\bar{Q}$ = mean peak discharge (in./h), and
A = drainage area in sq. mi.

Combining Eqs. (9), (10), and (11) (from Murphey et al. 1977), the equation corresponding to Eq. (6) is approximately

$$\bar{Q} = 5.06\bar{V}/\bar{D} \quad , \tag{12}$$

or $C_5 = 5.06$, which is quite close to the value of 4.82 found by Diskin and Lane (1976) in an independent analysis.

The procedure used was to compute runoff volume from the upland and lateral flow areas (using the hydrologic model for uplands), and then mean flow duration, using Eq. (9), and peak discharge, using Eq. (6). The runoff volumes are then taken as upland or lateral input into a channel segment for the routing calculations. As will be shown in the next section, estimates of mean runoff volume and mean flow duration are also used to compute transmission loss parameters for a channel segment.

Equations for the runoff volume at the end of a channel reach are derived, and then used with the peak discharge equation to estimate peak discharge. These equations thus estimate the influences of transmission losses on runoff volumes and rates.

In the absence of lateral inflow, if observed inflow/outflow data for a channel reach are related by regression analysis (Lane, Diskin, and Renard 1971), then an equation of the form

$$V(x,w) = \begin{cases} 0 & V_{up} \le V_o(x,w) \\ a(x,w) = b(x,w)V_{up} & V_{up} > V_o(x,w) \end{cases} \tag{13}$$

results, where

$a(x,w)$ = regression intercept (acre-ft or m^3),
$b(x,w)$ = regression slope,
$V_o(x,w)$ = threshold volume (acre-ft or m^3),
$V(x,w)$ = outflow volume (acre-ft or m^3),
V_{up} = inflow volume (acre-ft or m^3),
x = length of channel reach (mi. or km), and
w = average width of flow (ft or m).

When we set $V(x,w) = 0.0$, and solving for V_{up}, the threshold volume is

$$V_o(x,w) = \frac{-a(x,w)}{b(x,w)} \quad . \tag{14}$$

This is the inflow volume required before outflow begins. Inflow volumes less than $V_o(x,w)$ will all be lost or infiltrated into the channel alluvium.

Based on the preceding empirical observations and Jordan's work (1977) using an ordinary differential equation, Lane (1980) approximated the rate of change in runoff volume with distance as

$$\frac{dV}{dx} = -wc - wk\ V(x,w) \quad , \tag{15}$$

where c and k are parameters, and the other variables are as described above. The solution to Eq. (15) is

$$V(x,w) = \frac{-c}{k}\left[1 - e^{-kxw}\right] + V_{up}\, e^{-kxw} \quad , \tag{16}$$

where $V_{up} = V(x = 0,w)$ = the upstream inflow volume. By letting $x = w = 1$, Lane (1980) defined a unit channel, where $a(1, 1) = a$; $b(1, 1) = b$; and $c = -k(a/1 - b)$, so that Eq. (16) becomes

$$V(x,w) = \frac{a}{1 - b}\left[1 - e^{-kxw}\right] + V_{up}\, e^{-kxw} \quad . \tag{17}$$

Notice that if the following equivalence is made,

$$b(x,w) = e^{-kxw} \quad , \tag{18}$$

so that

$$a(x,w) = \frac{a}{1-b}[1 - e^{-kwx}] = \frac{a}{1-b}[1 - b(x,w)] \tag{19}$$

then Eq. (17) is identical to the regression model described by Eq. (13). Therefore, given observed inflow/outflow data for a channel reach, least squares analysis can be used to estimate parameters in the differential equation, Eq. (15), or its solution, Eq. (17).

If lateral flow areas contribute flow along the channel reach, and if this flow can be considered approximately uniform with distance along the channel reach, then Eq. (15) becomes

$$\frac{dV}{dx} = -wc - wk\,V(x,w) + V_{LAT/x} \quad , \tag{20}$$

where V_{LAT} is the lateral inflow volume. The solution to Eq. (20) is

$$V(x,w) = a(x,w) + b(x,w)V_{up} + \frac{V_{LAT}}{kwx}[1 - b(x,w)] \quad , \tag{21}$$

where a(x,w) and b(x,w) are defined by Eqs. (19) and (18), respectively. If the quantity [1 − b(x,w)]/kw is denoted F(x,w), then Eq. (21) becomes

$$V(x,w) = a(x,w) + b(x,w)V_{up} + F(x,w)V_{LAT/x} \quad , \tag{22}$$

where a(x,w), b(x,w), and F(x,w) are parameters to be determined for a particular channel reach.

The basic equation for the transmission loss model [Eq. (22)] involves upstream input (V_{up}), lateral inflow along the channel reach (V_{LAT}), stream segment length (x), channel width (w), and parameters a(x,w), b(x,w), and F(x,w). Given a runoff volume from Eq. (22), an estimate of the hydrograph shape parameter, and a mean flow duration, we use Eq. (6) to estimate peak discharge where the channel segments end. The procedure is repeated for each channel segment used to represent the channel system in a watershed. Each exterior channel segment receives input from an upland area and from lateral inflow along its reach coming from two lateral contributing areas. Each interior channel segment receives upstream inflow from one or two tributary channels and lateral inflow along its reach from two lateral contributing areas. The channel network and its contributing areas are used to represent the entire drainage basin or watershed.

III. ESTIMATING TRANSMISSION LOSS PARAMETERS

A. Equations and Techniques

Lane (1980) analyzed data representing 139 events from 14 channel reaches in Arizona, Texas, Kansas, and Nebraska. Based on these data, the unit channel parameters were estimated as

$$a = -0.00465K\bar{D} \tag{23}$$

and

$$k = -1.09\,\ln\,[1 - 0.00545K\bar{D}/\bar{V}] \quad , \tag{24}$$

where

- a = unit channel intercept (acre-ft),
- K = effective hydraulic conductivity (in./h),
- $\bar{D}$ = mean duration of flow (h),
- $\bar{V}$ = mean volume of flow (acre-ft), and
- k = decay factor $(ft/mi)^{-1}$.

When we use these parameter values, the transmission loss parameters are

$$b = e^{-k} \quad , \tag{25}$$

$$b(x,w) = e^{-kxw} \quad , \tag{26}$$

$$a(x,w) = \frac{a}{1-b}[1 - e^{-kxw}] = \frac{a}{1-b}[1 - b(x,w)] \quad , \tag{27}$$

and

$$F(x,w) = [1 - b(x,w)]/kw \quad . \tag{28}$$

Equations (23)-(28) define the transmission loss parameters to be used in the basic transmission loss model described by Eq. (22).

In addition to these analyses, data were obtained from 14 other channel reaches in Arizona (Wilson et al. 1980) and from seepage rates in unlined canals (Kraatz 1977). This information was used to derive estimates of effective hydraulic conductivity from alluvial characteristics, as summarized in Table VI.

The transmission loss component (as part of a basin-scale simulation model) was tested using data representing 222 runoff events from eight experimental watersheds on the Santa Rita Experimental Range near Tucson, Arizona. The model was also applied to predict annual flood series from 13 yr of data on a small watershed near Tombstone, Arizona, and for 30 yr of annual flood series on a small watershed near Safford, Arizona. The results of these analyses are summarized by Lane (1982a), wherein the model produced reasonable estimates of mean runoff volumes and peak rates and was used to simulate accurate flood frequency distributions.

Table VI. Effective Hydraulic Conductivity for Transmission Losses in Channel Alluvium[a]

Bed Material Group	Bed Material Characteristics	Effective Hydraulic Conductivity[b] (in./h)
1. Very high loss rate	Very clean gravel and large sand; $d_{50} > 2$ mm	>5.0
2. High loss rate	Clean sand and gravel under field conditions; $d_{50} > 2$ mm	2.0-5.0
3. Moderately high loss rate	Sand and gravel mixture with less than a few per cent silt and clay	1.0-3.0
4. Moderate loss rate	Sand and gravel mixture with significant amounts of silt and clay	0.25-1.0
5. Very low loss rate	Consolidated bed material with high silt-clay content	0.001-0.1

[a]Based on data analyses from 14 channel reaches in Arizona, Texas, Kansas, and Nebraska, from 14 other channel reaches in Arizona, and from canal seepage rates in unlined canals (Lane 1980).
[b]Values of effective hydraulic conductivity reflect the flashy sediment-laden character of many ephemeral streams, and thus do not represent steady-state rates of clear water infiltration.

Based on the transmission loss analyses summarized above (Lane 1980; 1982a), on the hydrograph analysis for semiarid watersheds (Murphey et al. 1977), and for subhumid watersheds (Lane et al. 1975), and on established hydrologic relationships (NEH-4 1972), parameter estimation techniques are summarized in Table VII.

Values of the duration-watershed area coefficient C_1 in Eq. (9) are shown in Fig. 2. The basin average curve number CN is the area-weighted average curve number for the watershed (NEH-4 1972), and it summarizes soil type, vegetation, and land use. The watershed length/width ratio, $L/W = L^2/A$, measures the relative length of the watershed with respect to the total drainage area. Low values of L/W usually indicate compact watersheds with efficient drainage systems. The exponent C_2 in Eq. (9) represents the rate of increase in mean flow duration with increasing watershed area; it varies from about 0.2 on semiarid watersheds to about 0.5 on more humid watersheds. We have no detailed hydrograph analyses suggesting a value for C_2, so we recommend using a C_2 in the range of 0.2 to 0.3.

Values of the mean volume-watershed area coefficient C_3 in Eq. (10) are shown in the upper portion of Fig. 3. The mean runoff volume per runoff event (in inches) varies with the basin average curve number. If all other factors are equal, the higher the curve number, then the higher the mean runoff volume per event. The exponent C_4 in Eq. (10) represents the rate of change in mean runoff volume per event with increasing watershed area. We have no long-term hydrologic data suggesting values for C_3 and C_4 in Eq. (10), so we recommend using the upper portion of Fig. 3 to estimate C_3 and using a C_4 value in the range -0.2 to -0.1.

Values of the hydrograph shape parameter C_5, representing the peak-volume relationship for a

Table VII. Parameters in the Transmission-Loss Streamflow-Routing Component

Parameter or Variable	Value Range	Estimate Source and Comments
Watershed Area A	--	Topographic map; drainage area contributes to the channel segment
Channel		
Length x	--	Topographic map and field observations
Width w	--	
Hydraulic conductivity K	0.001-5.0	Table VI or runoff data; function of channel alluvium, antecedent moisture, etc.
Hydrograph parameters		
C_1	2.5-5.0 0.2[a]	Fig. 2 in Murphey et al. 1977; or hydrograph analysis
C_2	0.5[b]	Murphey et al. 1977; or hydrograph analysis
C_3	0.03-0.07[a]	Fig. 3 in Murphey et al. 1977; or hydrograph analysis
C_4	−0.2[a] 0.0[b]	Fig. 3 in Murphey et al. 1977; or hydrograph analysis
C_5	3.0-5.0	Fig. 3 in Murphey et al. 1977; NEH-4 1972; or hydrograph analysis
$\bar{D}$	>0.0	$\bar{D} = C_1 A^{C2}$, mean flow duration (h)
$\bar{V}$	>0.0	$\bar{V} = C_3 A^{C4}$, mean runoff volume (in.); must convert to acre-ft

[a]Semiarid.
[b]Subhumid.

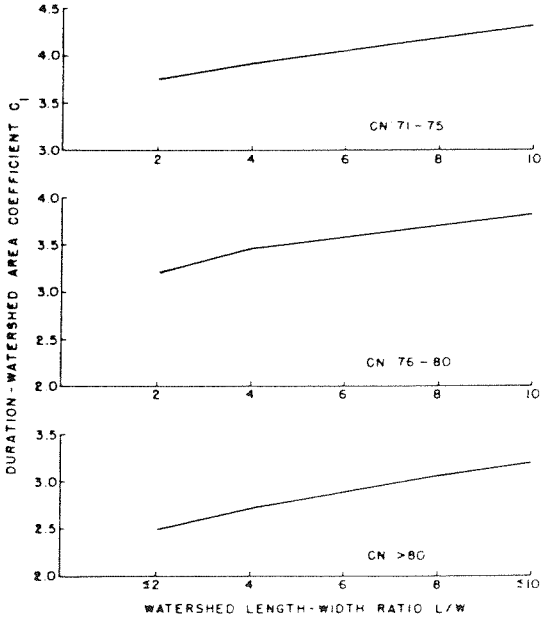

Fig. 2. Variation in duration-area coefficient C_1 as a function of basin average curve number CN and watershed length/width ratio L/W.

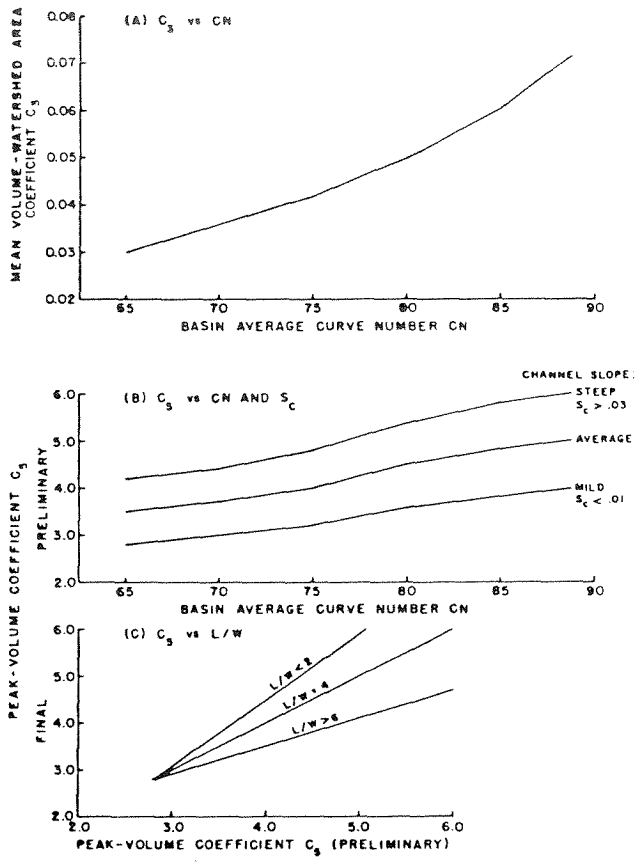

Fig. 3. Variation of coefficients with curve number (A), channel slope (B), and length/width ratio (C).

watershed, are shown in the central and power portions of Fig. 3. The basin average curve number measures flashy runoff, with higher curve numbers usually representing more rapid, and thus higher peaked runoff events, as shown in the central portion of Fig. 3 (NEH-4 1972). Watersheds with lower length/width ratios usually have a more compact and efficient drainage system, and thus produce higher peak rates of flow, as shown in the lower portion of Fig. 3. The procedure is to estimate C_5 as a function of CN using the central portion of Fig. 3 and to adjust this preliminary estimate, based on L/W, as shown in the lower portion of Fig. 3. Values of C_5 usually range from 3.5 to 4.5, but they can vary from less than 3.0 to over 5.0.

The parameter values shown in Table VII, Fig. 2, Fig. 3, and recommended in the preceding paragraphs should produce reasonable estimates for small rangeland watersheds, where streamflow is intermittent or ephemeral. However, if hydrologic data are available, hydrograph and regression analyses can be used to estimate values of effective hydraulic conductivity K and the hydrograph parameters C_1 to C_5.

Without observed hydrologic data, Table VII and Figs. 2 and 3 can still be used to estimate parameters for the hydrologic portion of the channel component. However, use judgment to ensure the believability of parameter estimates, so that the model will produce reasonable estimates of runoff rates and amounts. Although it is impossible to anticipate all circumstances, some general rules can be stated. The model is not intended for application in perennial streams or on watersheds where the runoff is dominated by snowmelt runoff. These include watersheds with significant baseflow, where the ground-water component dominates the streamflow. Generally, the model probably does not apply to watersheds where the mean annual precipitation is over 20 in., or where the mean annual runoff is much over 1.0 in.

The model is intended for application on small watersheds up to a few tens of square miles in size. For larger watersheds, to include a sufficient number of channel segments to accurately represent the drainage network is difficult. The model is intended to simulate runoff over a large range in storm size. However, during large storms, rivers may flow over the banks, so estimates must be adjusted to account for channel width and effective hydraulic conductivity during flow out of the banks.

B. Example Hydrographs

The routing procedure used herein assumes a characteristic hydrograph shape where the time to peak is 20% of the flow duration; the time to the inflection point on the recession is 40% of the flow duration; and the discharge at the inflection point is 20% of the peak discharge. The equations describing the double-triangle approximating hydrograph include:

$$\begin{cases} t = 0 & (29) \\ q = 0 \ , & (30) \end{cases}$$

$$\begin{cases} t = t_p = 0.2D & (31) \\ q = Q_p \quad , & (32) \end{cases}$$

$$\begin{cases} t_1 = 2t_p = 0.4D & (33) \\ q_1 = 0.2\ Q_p \quad , \text{ and} & (34) \end{cases}$$

$$\begin{cases} t = D & (35) \\ q = 0 \quad , & (36) \end{cases}$$

where D is the equivalent duration for the standard hydrograph shape [Eqs. (29)-(36)], the mean duration for the transmission loss equation is

$$\bar{D} = C_1 A^{C_2} \quad , \tag{37}$$

and the estimated peak discharge is

$$Q_p = C_5 V/\bar{D} \quad . \tag{38}$$

The quantity A in Eq. (37) is the drainage area in square miles above the channel segment; values of t are in hours; values of q are in inches per hour; and the quantity V in Eq. (38) is the runoff volume from the transmission loss equation [Eq. (22)]. When we integrate Eqs. (29)-(36), we find the runoff volume under the standard approximating hydrograph is

$$V = 7/25\ Q_p\ D = 1.4\ Q_p t_p \quad , \tag{39}$$

which means that the equivalent duration is given by

$$D = 25/7\ V/Q_p = 25/7\ \bar{D}/C_5 \quad , \tag{40}$$

where $\bar{D}$ is given by Eq. (37), and C_5 is given by the lower portions of Fig. 3. Equation (40) means that, when C_5 is less than 25/7 = 3.57, the equivalent duration for the standard approximating shape is greater than $\bar{D}$, and when C_5 is greater than 25/7, the equivalent duration is less than D. By using D from Eq. (40) in the standard approximating hydrograph, the volume V from Eq. (22) and the peak discharge Q_p from Eq. (38) are preserved or matched, but the hydrograph duration D is more or less than $\bar{D}$, depending on the ratio of 25/7 to C_5. Because C_5 varies from 6.0 to 2.8 (Table VII), the equivalent duration D is always in the range of 0.6D to 1.3D. The reason for adopting a standard approximating hydrograph for sediment routing in the channel is to be able to use a single piecewise normal approximating hydrograph, as discussed in a later section.

To summarize, the mean runoff volume for a channel reach [$\bar{V}$ in Eq. (10)] and the mean flow duration [$\bar{D}$ in Eq. (37)] are used in Eq. (22) to predict runoff volume and in Eq. (38) to predict peak discharge. Equation (40) is used to compute an equivalent flow duration for the standard approximating hydrograph [Eqs. (29)-(36)]. The standard approximating hydrograph is then used to represent the runoff hydrograph at the end of the channel segment. Effective hydraulic conductivity values are selected from Table VI, and the parameters C_1 through C_5 are selected from Table VII and Figs. 2 and 3. This parameter set and the appropriate equations are used to compute runoff volume, peak discharge, and an approximate hydrograph shape.

Hydrographs for drainage areas of 0.1, and 10.0 sq. mi. are shown in the upper portion of Fig. 4. In this example, an average CN of 80, an average channel slope, and a L/W of 4.0 were used in Figs. 2 and 3 to estimate C_1, C_5, and thus $\bar{D}$ and Q_p for a runoff volume of 1.0 in. The upper portion of Fig. 4 illustrates the influence of drainage area on the approximate hydrograph shape. The lower portion of Fig. 4 illustrates the influence of the basin average curve number on hydrograph shape. The upper portion of Fig. 5 illustrates the influence of the main channel's slope on the hydrograph shape, and the lower portion of Fig. 5 illustrates the influence of the watershed length/width ratio. Under typical conditions, as assumed in this example, Figs. 4 and 5 show that drainage area dominates hydrograph shape. Next in importance is the basin average curve number, followed by channel slope and watershed length/width ratio.

Transmission loss equations [Eqs. (22) and (38)] were used to route the hydrograph, shown in the upper portion of Fig. 6, in a channel segment with various hydraulic conductivity values. The routed hydrographs are shown in the lower portion of Fig. 6. In this example, there was no lateral inflow, and the outflow hydrographs were plotted on a common time scale.

Figures 4-6 show the influence of watershed characteristics and transmission losses on the shape and magnitude of the approximating hydrograph described by Eqs. (29)-(38). Although other factors affect the shape and magnitude of the runoff hydrographs, these examples illustrate that the

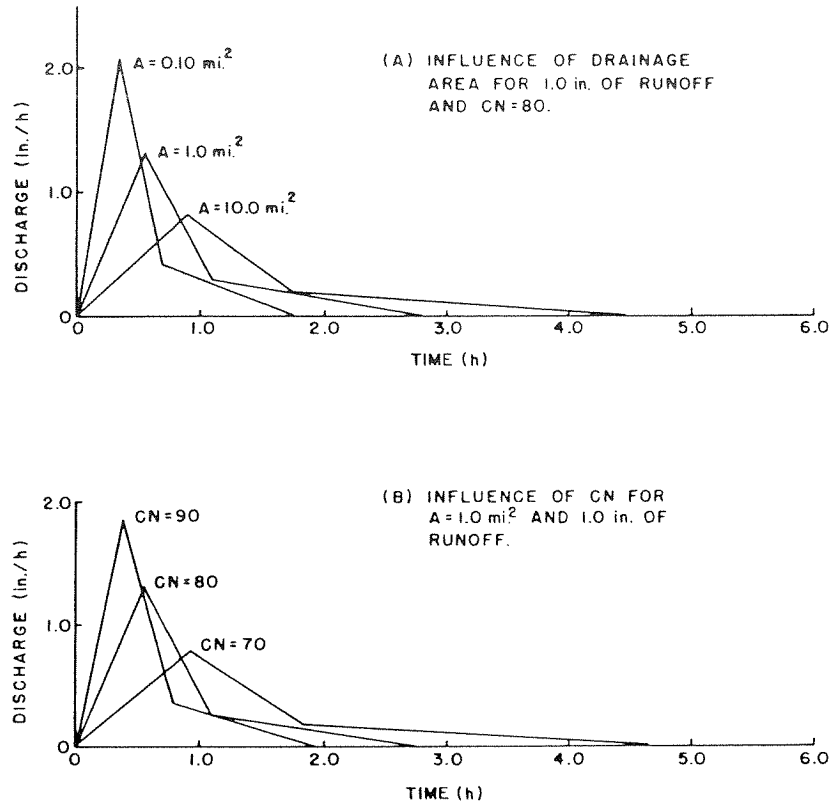

Fig. 4. Double-triangle approximating hydrographs for 1.0 in. (25.4 mm) of runoff illustrating (A) influence of drainage area and (B) influence of basin-average curve number on hydrograph shape.

model described herein accounts for many of the most important factors influencing runoff from semi-arid watersheds.

IV. OPEN-CHANNEL FLOW HYDRAULICS

The sediment transport calculations are based on two major hydraulic assumptions for simplicity in calculations; rectangular channel cross sections and of normal flow.

Under these conditions, the average flow velocity is given by the empirical Manning equation, which, in English units, is

$$V = \frac{1.49}{n} S^{1/2} R^{2/3} \quad , \tag{41}$$

where

V = average velocity (ft/s),
S = slope of the channel bottom,
R = hydraulic radius (in ft), and
n = Manning's roughness coefficient (in $s/ft^{1/3}$).

The hydraulic radius for a rectangular channel is

$$R = \frac{A}{WP} = \frac{WD}{W + 2D} \quad , \tag{42}$$

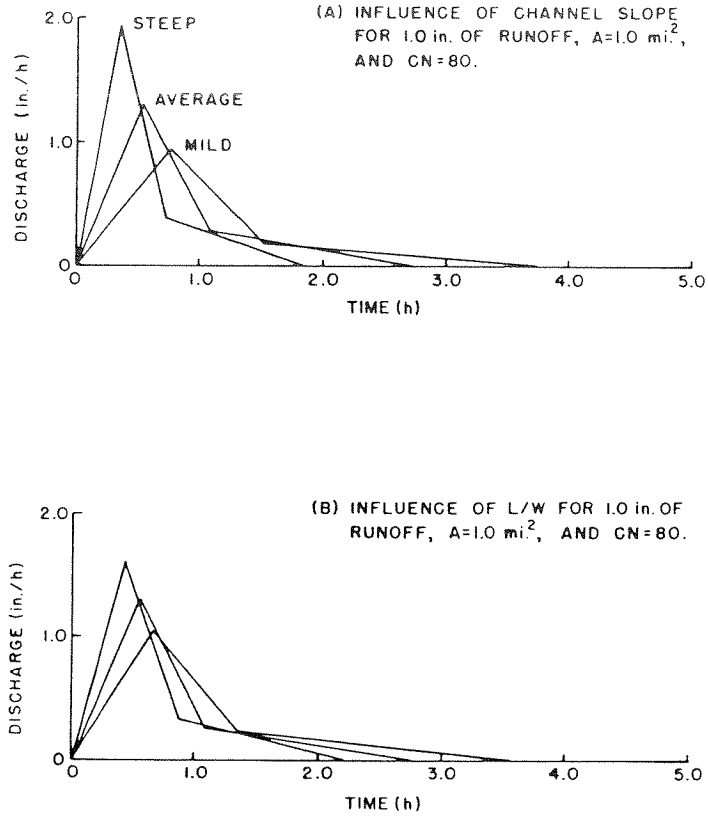

Fig. 5. Double-triangle approximating hydrographs for 1.0 in. (25.4 mm) of runoff illustrating (A) influence of channel slope and (B) influence of length/width ratio on hydrograph shape.

where

A = cross sectional area (in ft^2),
WP = wetted perimeter (in ft),
W = channel width (in ft), and
D = depth of flow (in ft).

The continuity equation is

$$Q = AV = WDV \quad , \tag{43}$$

where

Q = discharge rate (in cfs),
A = WD = cross-sectional area (in ft_2), and
V = average velocity (in ft/s).

The flow depth, which satisfies Eqs. (41) and (43), is called normal depth. Flow, where the depth is normal, is called normal flow.

A. Hydraulic Roughness

The roughness coefficient n in Eq. (41) has been tabulated for several channel types (Barnes 1967), and it represents the flow resistance provided by the channel bed and banks. This resistance or roughness is called the total roughness. Values of total roughness coefficients n_T for various channel types are shown in Table VIII.

B. Correction for Wall or Bank Roughness

Because the flow resistance contributed by the channel banks (wall roughness) is not directly involved in transporting sediment near the channel bed, its influence can be separated from the influence of the bed. Following Einstein (1942, 1944, 1950), the total cross-sectional area A_T is divided into an area pertaining to the wall A_w and an area pertaining to the bed A_b as

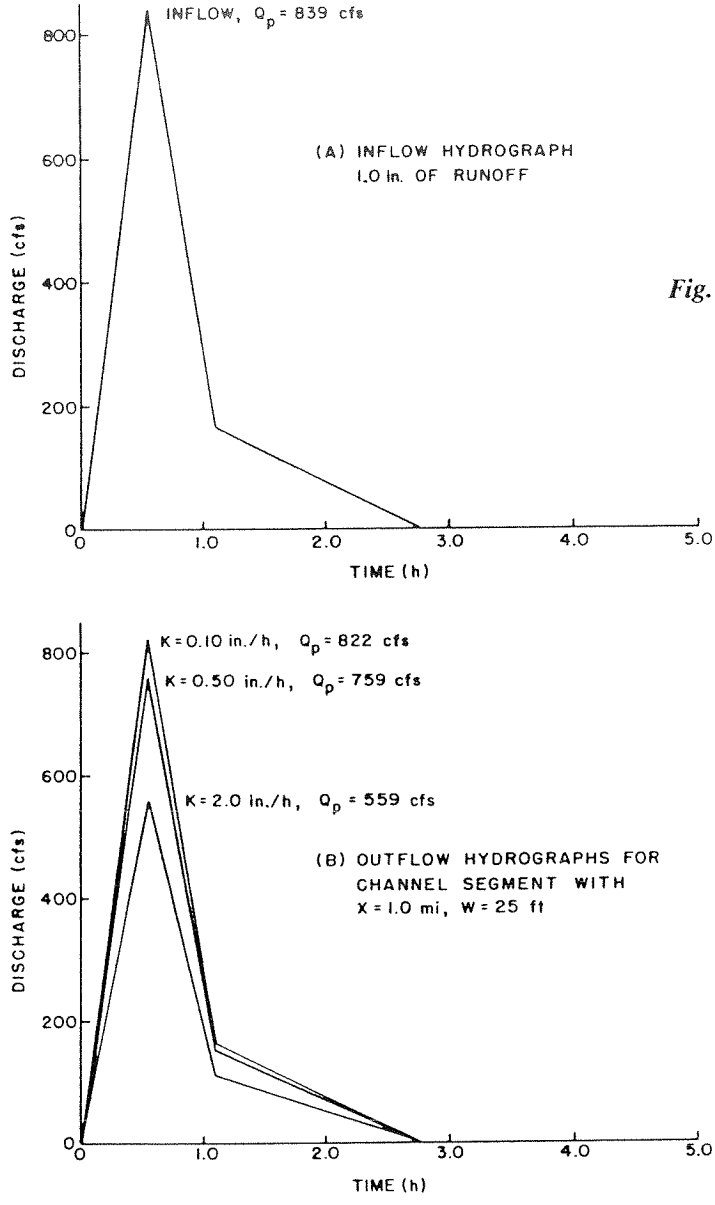

Fig. 6. Influence of transmission losses on inflow hydrograph for various values of effective hydraulic conductivity.

$$A_T = A_w + A_b \quad . \tag{44}$$

Now, if the energy gradient S and the velocity V are the same for the wall and bed, and the area is defined as the product of hydraulic radius and wetted perimeter, A = RWP, then Eq. (41) becomes

$$R_T(W + 2D) = R_w(2D) + R_b(W) \quad . \tag{45}$$

By the Manning equation, the hydraulic radius is

$$R = \left[\frac{Vn}{1.49S^{1/2}}\right]^{3/2} \quad , \tag{46}$$

where V is velocity and S is slope. Substituting Eq. (46) into Eq. (42), where V and S are common to all terms, produces

Table VIII. Approximate Hydraulic Roughness Coefficients for Open-Channel Flow (values are for the total roughness coefficient n_T)

Total Manning n, n_T	Channel Description
(0.02-0.10)	Excavated or Dredged Channels[a]
0.022	Earth, straight, uniform, and clean
0.027	Same, but with some short grass or weeds
0.025	Earth, winding and sluggish, with no vegetation
0.030	Same, but with some grass or weeds
0.080	Channels not maintained; weeds and some brush
(0.03-0.10)	Natural Streams[a]
0.030	Clean and straight; no rifts or deep pools
0.040	Clean and winding; some pools and shoals
0.048	Clean and winding; some weeds, stones, and pools
0.070	Sluggish reaches with weeds and deep pools
(0.012-0.040)	Wide, Alluvial Channels[b]
0.018-0.030	Ripples bed form, sediments finer than 0.6 mm, Froude Nos. <0.37
0.020-0.040	Dunes bed form, Froude Nos. 0.28 to 0.65
0.014-0.030	Transitional bed form, Froude Nos. 0.55 to 0.92
0.012-0.030	Antidunes bed form, Froude Nos. >1.0

[a]Source: Chow 1959.
[b]Sources: ASCE 1966; Simons and Richardson 1971.

$$n_T^{3/2}(W + 2D) = n_w^{3/2}(2D) + n_b^{3/2}(W) \quad , \tag{47}$$

and the solution for the hydraulic roughness of the bed n_b is

$$n_b = \left[n_T^{3/2} + \frac{2D}{W}\left(n_T^{3/2} - n_W^{3/2} \right) \right]^{2/3} \tag{48}$$

Geometric considerations suggest that the least value of R_b is ½ R_T, which means as a minimum

$$n_b \geq (1/2)^{2/3}\, n_T \tag{49}$$

and as a maximum

$$n_w \leq \left(\frac{W + 4D}{4D} \right)^{2/3} n_T \quad . \tag{50}$$

Equation (48) is evaluated for n_b subject to Eq. (49) as a constraint, which means that the hydraulic radius of the bed is

$$R_b = \left[\frac{V\, n_b}{1.49\, S^{1/2}} \right]^{3/2} \tag{51}$$

The procedure is to select a value of n_T from the second column in Table IX and a value of $n_w \geq n_T$ from the third column of Table IX. The computer program is written so that n_w must satisfy the constraint given by Eq. (50).

C. Correction for Grain

The grain, or particle resistance coefficient n_g is related to a representative grain size to the 1/6

Table IX. Approximate Hydraulic Roughness Coefficients for Total and Bank or Wall Roughness in Natural, Alluvial Channels[a]

Channel Description	Total, n_T	Wall, n_w
Upland Streams:		
Sand and gravel bed; bare exposed banks	0.030-0.040	0.030-0.045
Sand and gravel bed; exposed banks with some vegetation; grass and weeds	0.035-0.045	0.035-0.050
Sand and gravel bed, vegetated banks; grass and weeds with some brush	0.040-0.048	0.045-0.060
Wide, Alluvial Channels:		
Sand bed; bare, exposed banks	0.025-0.035	0.030-0.040
Sand bed, vegetated banks	0.030-0.040	0.035-0.050
Gravel bed, vegetated banks	0.030-0.040	0.035-0.050

[a]See Table VIII for values of n_T. In natural, alluvial channels, n_w is usually greater than n_T.

power (Strickler, 1923). This can be approximated as

$$n_g = 0.132(d_{50})^{1/6} \quad . \tag{53}$$

The hydraulic radius for grain resistance can then be estimated as

$$R_g = R_b\,(n_g/n_b)^{3/2} \quad , \tag{54}$$

where R_b is obtained from Eq. (51), and n_b is obtained from Eq. (48), subject to the constraints given by Eqs. (49) and (50).

D. Effective Shear Stress for Sediment Transportation

The effective shear stress for sediment transportation is given by

$$\tau = \gamma R_g S \quad , \tag{55}$$

where

τ = effective shear stress (lb/ft_2),
γ = specific water weight (lb/ft_3),
R_g = hydraulic radius for grain resistance (ft), and
S = energy gradient, slope of the channel bed for normal flow.

The effective shear stress, given by Eq. (55), will be less than the total shear stress averaged over the cross section $\gamma = \gamma R_T S$ because some of the total available energy is expended on the rough banks and some is expended on the rough bed.

V. HYDROGRAPH APPROXIMATION TECHNIQUES

Hydrographs in natural channels consist typically of a period of increasing discharge until the maximum or peak discharge is reached, then a period of recession or decreasing peak discharge, and finally, a longer period of gradually decreasing discharge. If the hydrograph is in an ephemeral stream, or if base flow is subtracted from the hydrograph, the resulting flood hydrograph starts at zero, rises to the peak, and returns to zero. Throughout this report, the term hydrograph refers to flood hydrographs of this type.

A. Double-Triangle Approximation

A continuous hydrograph representation is the double triangle, consisting of straight-line segments between the points given by Eqs. (29)-(36), as shown in Figs. 4-6. The equation describing this standard, double-triangle hydrograph is

$$q(t) = \begin{cases} (Q_p/t_p)t & 0 \le t \le t_p \\ 9/5\ Q_p - 4/5(Q_p/t_p)t & t_p \le t \le 2t_p \\ 1/3\ Q_p - 1/15(Q_p/t_p)t & 2t_p \le t \le 5t_p \end{cases} \quad (56)$$

where

q(t) = runoff rate (in./h),
Q_p = peak runoff rate (in./h),
t_p = time to peak = D/5 (h),
D = equivalent flow duration (h), and
t = time (h).

B. Piecewise Normal Approximation

The double-triangle hydrograph can be approximated by a series of step functions over the flow duration. If normal flow is assumed [Eqs. (41) and (43)] during each interval on the stepwise approximation, the result is a piecewise normal hydrograph approximation. Let t_i be the dimensionless time to the midpoint of an interval, let z_j be the length interval, and let u_j be the dimensionless ordinate for each interval. By our using nine intervals and the double-triangle hydrograph described by Eq. (56), the dimensionless hydrograph described in Table X results.

If each z_j is multiplied by the effective duration D and each u_j is multiplied by the peak discharge Q_p, the result will be a piecewise approximation to the double-triangle hydrograph, with duration D and runoff volume V. That is, the piecewise hydrograph matches the given runoff volume and effective duration exactly, and it approximates the peak discharge as $0.9Q_p$. Each interval length on the piecewise hydrograph equals z_jD and each discharge equals u_jQ_p. Within each interval, flow is assumed to be normal and thus satisfies Eqs. (41) and (43) through a numerical calculation subroutine; Eqs. (41)-(43), (48), (51), (54), and (55) are solved to estimate the hydraulic variables for the sediment transport calculations.

Table X. Values of the Dimensionless, Piecewise Approximating Hydrograph for Nine Intervals and the Standard Double-Triangle Hydrograph

Index (j)	Distance to Interval Midpoint (t_j)	Interval Length (z_j)	Dimensionless Hydrograph Ordinate (u_j)
1	0.050	0.10	0.250
2	0.125	0.05	0.625
3	0.175	0.05	0.875
4	0.225	0.05	0.900
5	0.275	0.05	0.700
6	0.350	0.10	0.400
7	0.500	0.20	0.167
8	0.700	0.20	0.100
9	0.900	0.20	0.033

C. Discussion

Development of a simplified hydrologic model has been described, which will compute runoff amounts and rates, runoff hydrographs, and hydraulic variables in ephemeral stream channels. The model is simplified to approximate these processes. Runoff volume, as a result of storm rainfall, is estimated using the SCS runoff equation. Hydrographs are represented by means of a procedure that accounts for drainage area influence, infiltration through the basin average curve number, main channel slope, and watershed shape through the length/width ratio. These watershed features are used to estimate the volume, peak discharge, flow duration, and thus the hydrograph shape for runoff delivered to the stream channel system. The complex processes controlling transmission losses are modeled with a linear differential equation, which includes length and width of the channel reach, effective hydraulic conductivity of the channel alluvium, and the mean values of flow duration and runoff volume. Note that all of these runoff variables and hydrograph features are calculated based on their average relationships with the watershed and channel features; the average relationships are then used to compute values for individual runoff events.

Because we based the hydrologic model on these average relations, predictions for individual events may be in error, especially for extreme events associated with very large or very small storms, or those associated with unusual antecedent conditions. As an example, flow duration is a function of antecedent conditions and storm size and duration. However, an average, or representative, flow duration is useful in predicting expected transmission losses and average peak discharge-runoff volume relations.

Runoff in natural stream channels is characteristically spatially varied and unsteady, but these variations in space and time are approximated by the piecewise normal hydrograph. Flowing water and the channel bed and banks interact

dynamically and produce complex open-channel flow relationships, represented by bed, bank, and grain resistance to flow in rectangular channels. These simplifications and assumed piecewise normal flow allow application of sediment transport equations to estimate sediment transport and yield.

VI. DEVELOPMENT OF THE SEDIMENT YIELD COMPONENT

Soil erosion, sediment transport and deposition, and sediment yield represent complex processes inasmuch as they depend on runoff rates and amounts, hydraulic variables, other climatic and watershed features, soil and sediment characteristics, and several dynamic interactions of the controlling processes. Ideally, all of these factors would be included in a mathematical model to predict sediment yield. However, as the area of interest extends from the upland areas to larger downstream areas, the processes occurring in stream channels become relatively more important. Features of the channel network or system can influence the runoff rates and amounts, as well as sediment yield. Under these conditions, we can develop some understanding and thus an approximate predictive capability, by emphasizing the influence of stream channel processes that partially control sediment yield.

A. Sediment Transport Calculations

Sediment transport is assumed equal to sediment transport capacity. If sediment load exceeds transport capacity, deposition occurs, and if transport capacity exceeds sediment load, scour or erosion may occur. However, for alluvial channels with noncohesive sediments, sediment transport rate is commonly assumed to be equal to sediment transport capacity. To avoid more elaborate sediment deposition models and channel erosion models (Foster et al. 1981), we assume in a first approximation that sediment transport rate and sediment transport capacity are equivalent.

Because sediment transport capacity is strongly related to localized, in-channel processes, it is largely determined by hydraulic variables. In-channel features, such as channel morphology and sediment properties, as well as the hydrologic and hydraulic variables, reflect upland processes, so these upland processes are reflected in the transport capacity calculations. That is, the channel system is part of the general landscape development.

B. The Bed-Load Equation

Following Einstein (1950) and others, we distinguish between bed load and suspended load. If we assume that sediment transport rate is proportional to the water flow rate, then this distinction is arbitrary, because particles that travel as bed load at one flow rate may be suspended at another. The relationship between transport model and flow rate is a dynamically complex one, and it represents a continuous rather than a distinct transition.

Nevertheless, we assume that the "larger" particles travel as bed load and that the "smaller" particles more easily enter suspension. Calculations are easier if we make a sharp distinction based on particle size. Therefore, we arbitrarily assume that all sediment larger than 0.062-mm in diameter is transported as bed load and that finer material is transported as suspended load. Separate transport equations were derived for bed-load transport and suspended-load transport, based on this assumption.

By using a modification of the Duboys-Straub formula (see Graf 1971 for a complete description), Lane (1982b) computed transport capacity for bed-load-sized particles,

$$g_{sb}(d_i) = \alpha f_i B_s(d_i)\tau[\tau - \tau_c(d_i)] \quad , \qquad (57)$$

where

$g_{sb}(d_i)$ = transport capacity per unit width for particles of size d_i,
α = a weighting factor to ensure that the sum of the individual transport capacities equals the total transport capacity computed using the median particle size,
f_i = proportion of particles in size class i,
d_i = diameter of particles in size class i (mm),
$B_s(d_i)$ = sediment transport coefficient (ft^3/lb-s),
τ = effective shear stress (lb/ft^2), and
$\tau_c(d_i$ = critical shear stress for particles in size class i (lb/ft^2).

Values of B_s and τ_c were determined by Straub (1935). The total bed-load transport capacity is then found by summing the results from Eq. (57) over all the size fractions.

However, values of B_s and τ_c, as developed by Straub (1935), were for total shear stress, rather than the effective shear stress, corresponding with

grain resistance. Lane (1982b) derived parameter estimates to be

$$B_s(d_i) = 40.0/(d_i)^{1.5} \quad (58)$$

and

$$\tau_c(d_i) = \begin{cases} 0.0022 + 0.010d_i , & 0.062 \leq d_i \leq 1.0 \\ -0.0078 + 0.020d_i & 1.0 < d_i \quad , \end{cases} \quad (59)$$

where d_i is the representative particle diameter (in mm). Equations (58) and (59) were calibrated with observed sediment transport data from the Niobrara River in Nebraska (Colby and Hembree, 1955) for particle sizes up to 2.0 mm. Therefore, Eqs. (58) and (59) have not been evaluated for particles larger than 2.0-mm diam. The weighing factor α in Eq. (57) ensures that the sum of the individual transport capacities equals the total transport capacity computed using the median particle size d_{50} in Eqs. (57)-(59). Consequently, the model has not been evaluated for values of d_{50} in excess of 1.0 mm.

C. The Suspended-Load Equation

Bagnold (1956, 1966) proposed a sediment transport model based on the concept of stream power,

$$i_s = P\frac{e_s u_s}{v_s}(1 - e_b) \quad , \quad (60)$$

where

i_s = suspended sediment transport rate per unit width (lb/s-ft),
$P = \tau V$ = available stream power per unit area of the bed (lb/s-ft),
e_s = suspended-load efficiency factor,
e_b = bed-load efficiency factor,
u_s = transport velocity of suspended load (ft/s), and
v_s = settling velocity of the particles (ft/s).

If u_s is assumed equal to the mean velocity of the fluid V then Eq. (60) is

$$g_{sus} = f_{sc} \cdot CAS \cdot \tau V^2 \quad , \quad (61)$$

where

g_{sus} = suspended sediment transport capacity (lb/s-ft),
f_{sc} = proportion of particles smaller than 0.062-mm diam in the channel bed material,
τ = effective shear stress (lb/ft_2),
V = average velocity (ft/s), and
CAS = suspended sediment transport coefficient (s/ft).

The suspended sediment transport coefficient CAS incorporates the efficiency parameters and the settling velocity of the suspended particles. CAS values have been determined by calibration with observed data. However, because data are scarce and the efficiency parameters and settling velocity interact with flow dynamics, CAS values are not well specified by measurable physical characteristics. Moreover, washload or sediment from the upland areas is transported through the channel system and may obscure the appropriate CAS value for fine sediments derived from the channel alluvium.

D. Calculation of Sediment Transport and Yield

1. Applications. Typical applications of the model's sediment transport component include predicting sediment discharge rates for steady flow and predicting sediment yields using the piecewise normal hydrograph approximation. The sediment transport model was fitted to data representing 27 observations at the Niobrara River in Nebraska (Colby and Hembree 1955). These data represent nearly steady-state conditions. Observed and computed sediment discharge rates are shown in the upper portion of Fig. 7. The fitted and measured sediment discharge rates agree very well.

The sediment yield model, using the piecewise normal approximation, was used to predict sediment yields for 47 runoff events from five small watersheds in southern and southeastern Arizona. These small (1.6- to 4.0-ha) watersheds are detailed by Lane et al. (1978). Predicted and observed sediment yields for these watersheds are shown in the lower portion of Fig. 7. Note the sediment yield data vary more than the sediment discharge data, and that the observed and computed data agree more

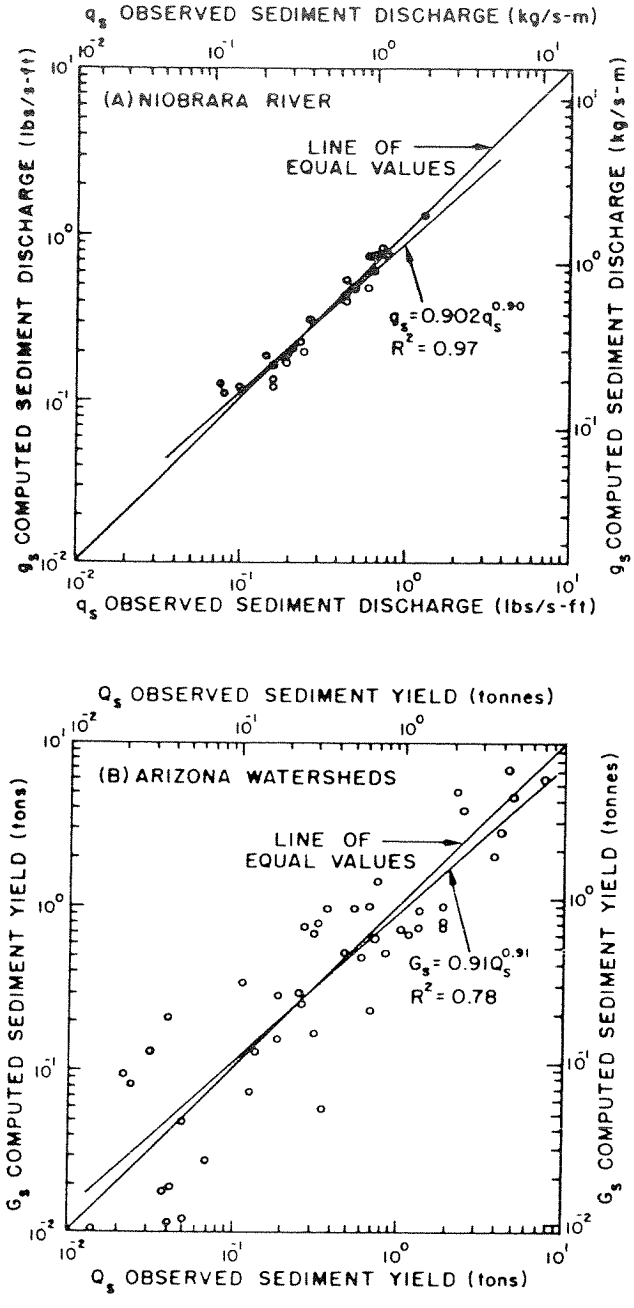

Fig. 7. Observed and computed sediment data for (A) the Niobrara River and (B) the Arizona watersheds.

closely when the model was calibrated (upper portion of Fig. 7) than when it was used to predict (lower portion of Fig. 7).

2. Parameter Estimation. We based our estimates on the sediment transport model summarized above (Lane 1982a, 1982b; and Lane and Hakonson 1982), the suspended transport model (Bagnold 1956, 1966), open-channel flow hydraulics (Chow 1959), and established sediment transport theory (Graf 1971), and our parameter estimation techniques are summarized in Table XI.

The channel width is not the mean representing average segment width in the transmission loss equations but is the actual channel width at the particular cross section where the sediment transport calculations are made. To meet the normal flow assumptions and the assumption that the channel bed material represents the sediment size distribution available for transport, the cross section should represent the assumptions and the particular channel reach. As much as possible, the cross section should reflect a straight reach with uniform flow conditions, uniform channel slope, and a representative sediment particle size distribution. The channel slope is the bed slope and should represent a uniform reach, as described above.

The sediment particle size distribution(f_i, d_i) should represent the sediment available for transport at the particular cross section and should not be biased by unrepresentative samples. Particles larger than those expected to be transported under anticipated flow conditions should be excluded from samples used to compute particle size distributions. The median particle size d_{50} is a critical parameter and should be based on enough representative samples to reflect the median size accurately. The proportion of silt-clay in the bed material f_{sc} is an equally important parameter, subject to the same sampling restrictions. Moreover, high values of f_{sc} will result in unrealistic proportions of silt-clay particles in transport. When the silt-clay proportion in the bed material f_{sc} exceeds a few per cent, the channel alluvium may change character from noncohesive to cohesive and may violate the model assumptions. Lacking better information, we recommend that the sediment model described herein should not be used if f_{sc} is greater than 0.10.

Take care while estimating the hydraulic roughness coefficients n_T and n_w, because they determine the velocity and effective shear stress under specified discharge rates and channel width and slope. All other factors being equal, higher values of the roughness coefficients result in lower sediment transport rates.

We estimated the transport parameters $B_s(d_i)$ and $\tau_c(d_i)$ from the representative particle diameter using Eqs. (58) and (59). As the particle diameter increases, $B_s(d_i)$ decreases and $\tau_c(d_i)$ increases. The combined result is a decrease in transport capacity

Table XI. Parameters in the Sediment Transport-Sediment Yield Component

Parameter or Variable	Value Range	Estimate Source and Comments
Channel:		
Width w	>0.0	Cross-section data; not the mean reach width as used in the transmission loss equations but actual width at the cross section of interest
Slope s	>0.0	Topographic map; field observations (Note: a very sensitive parameter, careful measurements must represent the channel at the point of interest)
Sediment:		
Particle size distribution (f_i, d_i)	$\Sigma f_i = 1 - f_{sc}$	Bed material samples; distribution of bed sediments larger than 0.062-mm
d_{50}	$0.062 \leq d_{50} \leq 2.0$ mm	Bed material samples; median particle size
f_{sc}	$0.0 < f_{sc} \leq 0.10$	Bed material samples; some bed material finer than 0.062 mm; f_{sc} values > 0.10 may indicate cohesive material
Hydraulics:		
Total roughness n_T	0.020-0.048	Table IX; field observations
Wall roughness n_w	0.030-0.060	Table IX; field observations
Transport parameters:		
$B_s(d_i)$	>0.0	Eq. (58)
$\tau_c(d_i)$	>0.0028	Eq. (59)
CAS	1.0-15.0	Suspended transport parameter; complex function of particle dynamics; estimate from calibration using observed data; default value, corresponding to medium-sized silt, CAS = 5.0 recommended

with increasing particle size. Finally, the transport parameter CAS is the least known and the most difficult to estimate from physical features of the sediment and flow dynamics. Preliminary relationships have been established, but without better information, we recommend using a value of 5.0 for CAS.

E. Discussion

Particle sorting and enrichment processes resulting from selective erosion, transport, and deposition are modeled by sediment transport equations for suspended particles and those in up to 10 class intervals in the bed-load range. By including discharge variations throughout the hydrograph and transport capacity variations through the range of particle sizes, the transport calculations simulate the particle-sorting processes. We used the piecewise normal approximating hydrograph and the particle size distribution for bed sediments, so the sediment yield calculations include the influence of particle-sorting processes on sediment yield.

As in the hydrologic model, observed data can help determine parameter values for the sediment yield component, or they can help improve the accuracy of the parameter estimates. However, in the absence of observed data, the relationships presented herein can be used to estimate the model parameters.

Once the model is applied to a particular watershed-channel system, we can use it to derive statistical relationships such as sediment rating curves, delivery ratios, and enrichment ratios. These relationships, in turn, can be used to predict sediment yield, to characterize the particular watershed, and to compare it with other watersheds.

VII. DEVELOPMENT OF A CONTAMINANT TRANSPORT MODEL

Many contaminants are transported and redistributed in the environment because of surface runoff and sediment yield. For these contaminants, if we can predict runoff and sediment yield as the driving force and transport mechanism, then we should be able to predict contaminant transport rates. Many contaminants, such as the actinides in general and plutonium in particular, are strongly associated with soils and sediment. Under these circumstances, if we can predict sediment yield, then we can begin to explain varying contaminant transport rates because of variations in sediment transport rates.

A. Transport of Sediment-Associated Contaminants

Differential erosion, transportation, and deposition result in sediment particle sorting. Because these processes are selective as a function of particle size and characteristics, transported sediment is usually enriched in finer sized particles. Because of physico-chemical processes that relate to particle size and characteristics, contaminants can be more strongly associated with the smaller sediment particles than they are with the larger sediment particles. The combined processes of particle sorting and differential association of contaminants by sediment particle size can produce contaminant enrichment in the transported sediment.

B. An Approximate Enrichment Ratio

A traditional approach to estimating transport rates for a particle-associated contaminant is to use an enrichment ratio (see Massey and Jackson, 1952), whereby contaminant flux Q_c is estimated at

$$Q_c = ER\, C_s\, Q_s \quad , \tag{62}$$

where:

Q_c = contaminant discharge rate (M/T),
ER = enrichment ratio,
C_s = mean concentration of soil contaminant, and
Q_s = sediment discharge rate (M/T).

If contaminant concentration and sediment transport rates are available by particle size classes, then we can write

$$Q_c = \sum_{i=1}^{N} C_s(d_i)\, Q_s(d_i) \quad , \tag{63}$$

where

Q_c = contaminant discharge rate (M/T),
$C_s(d_i)$ = contaminant concentration associated with particles in size class i,
d_i = representative particle diameter in size class i (mm),

$Q_s(d_i)$ = particle transport rate in size class i (M/T),
i = index for the sediment particle size class, and
N = number of size classes in the sediment mixture.

The mean contaminant concentration C_s in Eq. (62) can be defined as

$$C_s = \sum_{i=1}^{N} f_i C_s(d_i) \quad , \tag{64}$$

where f_i is the proportion of the channel bed material in size class i, and the variables are as defined above. Equating Eqs. (62) and (63) with C_s as defined in Eq. (64), we solve the enrichment ratio from

$$ER = \frac{\Sigma C_s(d_i) Q_s(d_i)}{Q_s \Sigma f_i C_s(d_i)} \quad , \tag{65}$$

where the summations are over the N-sized classes. Equation (65) describes an enrichment ratio for sediment-associated contaminants in channel alluvium, which are transported as described by the sediment transport equations. Equation (65) defines an enrichment ratio to use in Eq. (62), or Eq. (63) can be used directly. In any event, Eqs. (62), (64), and (65) describe the influence of sediment particle sorting on contaminant enrichment in streamflow.

Equations (62) and (63) are for discharge rates at a particular time. If we integrate over an entire runoff event, through the piecewise normal hydrograph, similar relationships can be derived in terms of total sediment yield. In this case, the enrichment ratio and other variables will be constant for the entire runoff event and associated sediment yield, rather than for a particular instantaneous rate.

C. Approximate Values for Enrichment Ratios

Recently, Watters et al. (1982) compiled enrichment ratios for several elements at various locations in the United States from a survey of literature. These data are summarized in Table XII.

Although the enrichment ratio data in Table XII were collected under many circumstances, they represent typical values and their range or variability about the mean values.

VIII. A SIMPLE MASS-BALANCE-INVENTORY CALCULATION

When a sediment-associated contaminant is introduced directly into a channel system and is thus associated with the channel bed sediments, we can write a mass-balance equation. A mass-balance equation for a particular channel reach and for a particular time period is

$$\frac{dM}{dt} = I - kQ_sM \quad , \tag{66}$$

where

dM/dt = time rate of change in contaminant mass (M/T),
I = contaminant inflow or input rate (M/T),
k = coefficient (M^{-1}),
Q_s = sediment yield per unit time (M/T), and
M = contaminant mass (M).

The coefficient k, multiplied by the contaminant mass M, is expressed in units of concentration and can thus incorporate the dimensionless enrichment ratio described earlier. Equation (66) states that the rate of change in contaminants stored in a channel reach equals the difference between input to the reach and output from the reach. In this case, output from the reach is calculated from contaminant transport associated with sediment yield. For subsequent downstream channel reaches, the input to the reach is the outflow from the previous reach. In this way, we can route contaminants through an entire channel network model, and the total amount of stored contaminant is found by summing the contaminant mass M over all channel reaches in the channel network.

IX. PRELIMINARY EVALUATION OF SIMULATION RESULTS

When the simulation model is applied to watersheds where observed runoff, sediment, and contaminant yield data are available, the simulation results should be compared with observed data. However, if observed data are unavailable, or when they represent short or limited observations, we should still assess the accuracy of the simulation results. Although it is not possible to really assess the accuracy of simulation results under these conditions, we can compare the simulation results with

Table XII. Approximate Enrichment Ratios for Nutrients and Plutonium Associated with Sediment (Watters et al., 1982)

Land Use and Location	Approximate Enrichment Ratio		Comments
	Mean	Range	
Cropland, USA[a]	4.5	2.5-7.4	Nitrogen
	3.6	2.6-6.0	Phosphorus
Rangeland, USA[a]	2.6	1.1-6.7	Nitrogen
	7.1	2.7-17	Phosphorus
Cropland, USA[b]	1.6	1.1-2.5	Fallout plutonium
Pasture, USA[b]	2.3	0.8-4.0	Fallout plutonium
Mixed cropland, USA[c]	2.5	1.2-4.0	Fallout plutonium transport in perennial river
Semiarid, USA[d]	5.5	1.4-13.3	Waste effluent plutonium transport in ephemeral streams

[a]Small agricultural watersheds (5.2-18 ha) at Chickasha, Oklahoma.
[b]Small agricultural watersheds (2.6-2.9 ha) near Lebanon, Ohio.
[c]Great Miami River (drainage area = 1401 km^2) at Sidney, Ohio.
[d]Los Alamos watersheds (176-15 000 ha) near Los Alamos, New Mexico.

somewhat generalized empirical relationships. These comparisons should provide a preliminary assessment of the simulation model's performance, and should help to identify possible errors in estimating the parameter values.

The National Weather Service publishes a precipitation frequency atlas containing estimates of rainfall depths for various durations and return periods (Miller et al. 1973). In a particular location, rainfall depths expected to occur in a given time period (1 h, 2 h, 24 h, etc.) can be estimated for various return periods (2 yr, 10 yr, etc.). Data for Los Alamos, New Mexico, are shown in Table XIII. Simulated flood frequency estimates can be derived by running the hydrologic model with rainfall frequency data (such as in Table XIII) to estimate flood peaks for various return periods. In the runoff simulations, Eq. (9) can be used to estimate a mean flow duration $\bar{D}$ in hours; then 20% of this mean duration can be taken as an equivalent storm duration. For example, if $C_1 = 3.5$ and $C_2 = 0.2$, the mean flow duration for a 10-mi.^{2} watershed is $\bar{D} = 3.5(10)^{0.2} = 5.55$ h, or 330 min. Taking 20% of this duration results in a 66-min estimated storm duration. Therefore, as a first approximation, we would suggest using the 60-min rainfall depths from Table XIII to derive a flood frequency curve for a 10-mi.^{2} watershed at Los Alamos, New Mexico.

Selected criteria for preliminary evaluation of model simulation results are summarized in Table XIV. Simulated flood frequency curves can be derived and compared with regional flood frequency estimates from the U.S. Geological Survey (for example, see Dalrymple, 1965) or other sources. We suggest plotting normalized flood peaks (in cubic feet per second per square mile or cubic meter per second per square kilometer) against the return period using simulated and regional measured data. We can thus visually compare the simulated peak discharge rates per unit area with those measured in the region surrounding the particular watershed of interest. If the simulated and observed flood frequency distributions differ greatly, we may need

Table XIII. Precipitation Frequency Estimates for Los Alamos, New Mexico
(106°19′ W, 35°52′ N, elev = 7410 ft)
from Precipitation Frequency Atlas, "NOAA Atlas-2"
(Miller et al. 1973)[a]

Return Period	Estimated Rainfall Depths, in Inches, for the Given Time Period and the Given Return Period							
Tr (Years)	15-min P_{15}	30-min P_{30}	60-min P_{60}	2-h P_2	3-h P_3	6-h P_6	24-h P_{24}	Annual[b] P_A
2	0.56	0.77	0.98	1.11	1.20	1.36	1.76	17.99
5	0.72	1.00	1.26	1.42	1.53	1.74	2.32	24.06
10	0.82	1.13	1.43	1.62	1.75	2.00	2.67	25.79
25	0.95	1.31	1.66	1.89	2.04	2.32	3.14	27.9[c]
50	1.07	1.49	1.88	2.13	2.30	2.61	3.57	29.0[c]
100	1.19	1.64	2.08	2.36	2.55	2.90	4.00	30.24

[a]Source: J. F. Miller, R. H. Frederick, and R. J. Tracey, "NOAA Atlas-2, Precipitation-Frequency Atlas of the Western United States, Volume IV - New Mexico," U.S. Dept of Commerce, NOAA, National Weather Service, Silver Spring, Maryland (1973).
[b]Source: W. V. Abeele, M. L. Wheeler, and B. W. Burton, "Geohydrology of Bandelier Tuff," Los Alamos National Laboratory report LA-8762-MS (October 1981).
[c]Interpolated values.

Table XIV. Selected Criteria for Preliminary Evaluation of the Model Simulation Results

Component/Processes	Criteria/Comments
Hydrologic Model:	
Flood frequency analysis	Regional flood frequency curves; compare simulated flood frequency with regional values
Runoff drainage area	Plot runoff volume and peak discharge vs drainage area for given return period floods; evaluate exponents
Sediment Yield Model:	
Discharge-concentration relationships	Compare with empirical sediment-rating curves
Sediment yield-drainage area	Compare with empirical delivery ratios
Contaminant Transport:	
Enrichment ratios	Compare with empirical enrichment ratios
Mass balance	Check the mass balance and inventory

to adjust the parameter estimates in the hydrologic model.

Limited sensitivity analyses (Lane 1982a) show that hydrologic model results are most sensitive to runoff curve number, rainfall depth, and effective hydraulic conductivity. First, the user should review the data presented in Tables II-V to verify the CN estimates, and in Table VI to verify the estimates of effective hydraulic conductivity. Next, we would suggest reviewing Table VII and Figs. 2-5 for the estimates of C_1-C_5. Changes in these parameters might require re-estimating the effective storm duration.

Specific relationships for the other criteria listed in Table XIV are shown in Table XV. Once the flood frequency estimates are judged to be reasonable, we can examine other derived relationships. To compare simulated runoff variables with the empirical criteria summarized in Table XV, we recommend using simulated runoff for particular flood frequencies. In some cases, the mean annual flood (the flood corresponding with 2-yr rainfall depths as shown in Table XIII) may be appropriate. However, in low-runoff areas with significant transmission losses, the 2-yr flood estimates may vary, with transmission losses masking runoff/drainage area relationships. Under these circumstances, the 5- and 10-yr flood estimate may be more appropriate. In general, we recommend using the 2-yr flood estimate for deriving runoff-drainage area relationships to compare with the empirical relationships shown in Table XV. Although unusual circumstances can occur, if the exponents C_4 and C_7 are outside the probable ranges shown in Table XV, we suggest a careful examination of the input parameters. We may also compare the derived relationships for the 50- or 100-yr floods with the empirical relationships shown in Table XV to determine how the model performs with extreme values of the rainfall input.

If the hydrologic model is providing reasonable runoff estimates, we can compare computed sediment concentration with water discharge rates. By selecting discharge rates from the piecewise normal hydrograph approximation and comparing them with corresponding sediment concentration estimates (for example, with the 18 discharge rates represented by the 2-yr and 100-yr flood hydrographs), a relationship, $C = C_8\, q^{C_9}$, can be derived as shown in the central portion of Table XV. If the exponent C_9 falls outside the probable range shown in Table XV, we suggest reviewing Tables IX and XI to verify the parameter estimates. If the value of C_9 is less than zero, or near zero, the estimated channel width may be too narrow to represent hydraulic relationships in the natural channel, or the wall roughness esimates may be too high, or both. If so,

Table XV. Evaluation Criteria for Model Simulation

Process	Relationship	Comments
Runoff volume-Drainage area	$V = C_3 A^{C_4}$ (in., sq. mi.)	Probable range of C_4: $-0.2 \leq C_4 \leq 0.0$
Peak discharge-Drainage area	$Q = C_6 A^{C_7}$ (in./h, sq. mi.)	Probable range of C_7: $-0.5 \leq C_7 \leq -0.3$
Sediment concentration-Discharge rate	$C = C_8 q^{C_9}$ (—, cfs)	Probable range of C_9: $0.0 \leq C_9 \leq 1.0$
Sediment yield-Drainage area	$Y = C_{10} A^{C_{11}}$ (Tons/sq. mi., sq.-mi.)	Probable range of C_{11}: $-0.50 \leq C_{11} \leq 0.0$
Contaminant	---	Probable range of ER:
Enrichment ratio ER, Mean value		$2.0 \leq ER \leq 6.0$

we recommend plotting the depth-discharge relationship for the natural channel, and comparing it with the depth-discharge relationship for a rectangular channel with the assumed width. It may be necessary to adjust the rectangular channel width until the natural channel and rectangular channel depth-discharge relationships are in better agreement. If the exponent C_9 is greater than 1.0, we suggest checking the roughness estimate, the particle size estimates, and the channel slope estimate.

As in the case for runoff-drainage area relationships, we recommend using the 2-yr flood to estimate total sediment yield as a function of drainage area. Normalized sediment yield (in tons per square mile or metric tons per square kilometer) should be plotted against drainage area to determine the exponent C_{11}. Values of C_{11} should fall within the probable range shown in Table XV. If C_{11} is outside the probable range, parameter estimates from Table XI should be reviewed and adjusted if they are in error or outside the specified value range.

Finally, computed enrichment ratios should be compared with the probable range, as shown in Table XV. If the computed enrichment ratio is outside the probable range, then we suggest reviewing the particle size estimates, particularly the proportion of material finer than 0.062-mm diam.

Although the preliminary evaluation criteria are arbitrary and empirically based, they reflect our recommendation for a preliminary assessment of how well the model is performing in a particular application, especially when the application is on an ungaged watershed with insufficient data to analyze the accuracy of the simulation results.

If the procedure described above is followed, and the simulation results agree with the empirical criteria outlined in Tables XIV and XV, the model is not necessarily reproducing processes accurately that occur in the actual watershed. Instead, the model is probably operating as it was intended to operate, and thus is probably reflecting the physical processes that are represented by the equations included within the model structure and their representations that are limited by our abilities to parameterize these equations. Intentionally, and of necessity, the model is structured to represent simplified average relationships between watershed characteristics, rainfall, runoff, sediment, and contaminant yields.

X. APPLICATIONS AT LOS ALAMOS, NEW MEXICO

Los Alamos is located about 100 km north-northeast of Albuquerque, New Mexico. The Los Alamos National Laboratory is on the Pajarito Plateau, which ranges in elevation from 1800 m near the Rio Grande to about 2400 m on the east flank of the Jemez Mountains. Climate varies from an arid continental climate, near the Rio Grande, to semiarid continental mountain climate in the remainder of the Pajarito Plateau. Mean annual precipitation varies with elevation, from about 240 mm near the Rio Grande, to over 500 mm at the upper elevations of the plateau near the mountains, with correspondingly higher values in the Jemez Mountains. The annual mean minimum temperature at Los Alamos is about −4°C, and the corresponding mean maximum is about 22°C.

On an areal basis, some 60% of the soils in Los Alamos County were derived from Bandelier Tuff composed of ashfall, ashflow pumice, and rhyolite tuff deposited as a result of a volcanic eruption in the Jemez Mountains. The tuffs adjoin older volcanics of the Tschicoma Formation near the Jemez Mountains, and this formation accounts for an additional 20% of the soil mapping unit in Los Alamos County. Detailed soil survey data are given by Nyhan et al. 1978 and Griggs 1964.

Although as many as seven major overstory vegetation types are described in the soil survey data, we will consider only the three main types: (1) piñon-juniper woodland in roughly the lower third of the plateau, (2) ponderosa pine forest/piñon-juniper woodland in roughly the central third of the plateau, and (3) ponderosa pine-fir, fir, and fir-aspen in the upper areas of the plateau and the Jemez Mountains (Nyhan et al. 1978).

Los Alamos Canyon heads into the Jemez Mountains and cuts into the surface of the Pajarito Plateau. Except for the upper reaches, near the mountain front, streamflow is intermittent. Generally, the stream channels are narrow and incised in the upper reaches, and broader and more ephemeral in the lower reaches. The relative importance of transmission losses into the channel alluvium increases in the downstream direction. Major tributaries are Acid-Pueblo Canyon and Bayo Canyon from north of Los Alamos Canyon. Farther

downstream, Los Alamos and Guaje Canyons combine for about 2.4 km before reaching the Rio Grande (Fig. 8).

A. Operations, Waste Disposal, and Contaminants

Details on site operation, waste treatment and disposal, and contaminant types and concentrations were summarized by Stoker et al. (1981). The following material (without references to specific figures and tables) is excerpted from Stoker et al. (1981, pp. 10-11) to provide a brief description of waste disposal operations.

> "The radioactive liquid wastes resulted from work starting in 1943 as part of the U.S. Army's secret Manhattan Engineer District to develop a nuclear fission weapon and carried on after 1947 under auspices of the AEC as the Los Alamos Scientific Laboratory. Los Alamos was selected in November 1942 as the site for Project Y. The War Department acquired the Los Alamos Ranch School with 54 buildings and about 14.6 km^2 of school and other private holdings. About 186 km^2 of additional land were acquired from other government agencies with the total land filling out essentially all of what is in the present-day Los Alamos County. The first construction contract was let in December 1942, and in January 1943 the University of California assumed responsibility for operating the Laboratory. The first technical facilities known as the Main Technical Area or TA-1 were constructed on about 0.16 km^2 near the existing Ranch School facilities around Ashley Pond and along part of the north rim of Los Alamos Canyon. Buildings in which general laboratory or process chemistry and radiochemistry wastes were produced, were served by industrial waste lines known as acid sewers. Ultimately, all such industrial wastes flowed into a main acid sewer that extended generally north to a discharge point at the edge of Acid Canyon.
>
> "The untreated liquid wastes were discharged starting in late 1943 or early 1944 and continued through April 1951. These effluents contained a variety of radioactive isotopes from the research and processing operations associated with nuclear weapons development. No detailed analyses are available but it is known that radioactivity of interest included isotopes of strontium, cesium,

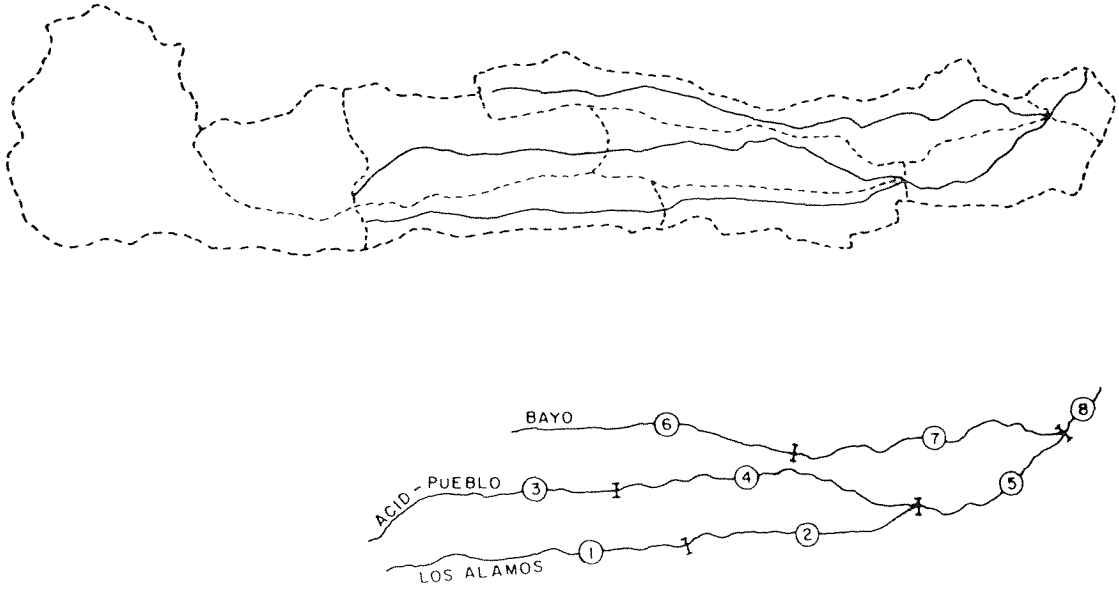

Fig. 8. Los Alamos Canyon drainage area and main channel network.

uranium, plutonium, americium, and tritium.

"In 1948 a joint effort was started with the U.S. Public Health Service to develop a method for removing plutonium and other radionuclides from radioactive liquid waste. Bench-scale experiments showed that conventional physico-chemical water treatment methods could be modified for treatment of radioactive waste. By June 1951 a treatment plant (identified as TA-45) had been designed, constructed, and began processing the radioactive and other laboratory wastes by a flocculation-sedimentation-filtration process.

"From startup until mid-1953, the TA-45 plant treated liquid wastes from only the original Main Technical Area, TA-1. Starting in June 1953, additional radioactive liquid wastes were piped to TA-45 from the new laboratory complex (TA-3) south of Los Alamos Canyon, which included the Chemistry and Metallurgical Research building where plutonium research was conducted. In September 1953, liquid wastes from the Health Research Laboratory (TA-43) were added to the system. Initially the TA-3 waste was very dilute, and a practice was adopted of monitoring the levels to determine if treatment was required to maintain the 2-week effluent average from TA-45 below 330 disintegrations/min/ℓ (the level adopted from National Bureau of Standards Handbook 52, Ref. 4, as the administrative level for effluent release from TA-45). If treatment was not required to meet the criteria, the TA-3 waste was discharged untreated to Acid Canyon. By December 1953, only about 30% of the TA-3 waste was released untreated. In 1958, liquid wastes from a new radiochemistry facility (TA-48) were added to the line coming from TA-3. The wastes from this facility included primarily fission products and are reflected in the higher gross beta and gamma content of the TA-45 effluents.

"In July 1963, the wastes from TA-3 and TA-48 were redirected to a new Central Waste Treatment Plant (TA-50) located south of Los Alamos Canyon within the present Los Alamos National Laboratory site. The liquid wastes from TA-43 were redirected to the sanitary sewer because only small quantities of very low concentration wastes were generated by that time. Subsequently, only liquid wastes from TA-1 were processed at TA-45 until it ceased operation near the end of May 1964. Some untreated low level liquid wastes containing some fission products from decommissioning of Sigma Building at TA-1 were released until June 1964. After this time no further effluents were released into Acid Canyon.

"Other releases have been or continue to be made into Pueblo and Los Alamos Canyons that have some bearing on the interpretation and assessment of the measurements of residual contamination in these canyons. Nonradioactive effluents include those released into Pueblo Canyon from three sanitary waste treatment plants, two of which continue in operation under the management of Los Alamos County. Radioactive effluents are those from the radioactive liquid waste treatment plant still serving TA-21 on the Los Alamos National Laboratory site. Effluents from this plant are released into DP Canyon, a small tributary to Los Alamos Canyon. This treatment plant started operations in June 1952 to serve the old plutonium processing facility that is now undergoing decontamination for conversion to other uses. The plant may treat wastes from new operations at TA-21, but levels of plutonium and americium are expected to decline. Some residuals from these treated effluents are carried into and down Los Alamos Canyon."

Acid-Pueblo Canyon received unknown amounts of radioactive wastes from 1943 to 1964, and DP-Los Alamos Canyon received various amounts of treated radioactive wastes from 1952 to 1980. The major emphasis in this report is on the transport and distribution of plutonium. Therefore, waste discharge data for plutonium are summarized in Table XVI.

The discharges of effluent into upper Acid-Pueblo Canyon from 1951 through 1964 are well documented in comparison with discharge amounts

Table XVI. Estimated Discharges of Plutonium in Stream Channels on the Los Alamos National Laboratory (Discharges are in terms of activity measured in millicuries of plutonium isotopes)

Year	Effluent Discharge (in mCi)	
	Upper Acid-Pueblo	Upper DP-Los Alamos
1943	18.75 to 375	0.0
1944	18.75 to 375	0.0
1945	18.75 to 375	0.0
1946	18.75 to 375	0.0
1947	18.75 to 375	0.0
1948	18.75 to 375	0.0
1949	18.75 to 375	0.0
1950	18.75 to 375	0.0
1951	1.3	0.0
1952	1.1	1.27
1953	1.2	1.27
1954	2.2	1.27
1955	2.2	1.27
1956	1.1	1.27
1957	0.9	1.27
1958	0.9	1.27
1959	1.2	1.27
1960	2.6	1.27
1961	5.3	1.27
1962	3.9	1.27
1963	3.0	1.27
1964	0.04	1.27
1965	0.0	1.27
1966	0.0	1.27
1967	0.0	1.27
1968	0.0	1.27
1969	0.0	1.27
1970	0.0	1.27
1971	0.0	1.27
1972	0.0	1.27
1973	0.0	1.27
1974	0.0	1.27
1975	0.0	1.27
1976	0.0	1.27
1977	0.0	1.27
1978	0.0	0.54
1979	0.0	0.14
1980	0.0	0.045

from 1943 to 1951. During this earlier period, an unknown amount of activity was introduced into Acid Canyon. Some estimates ranged as low as 150 mCi (Stoker et al. 1981, p. 26). However, inventory estimates, based on analysis of plutonium concentration data from sediment samples collected during surveillance activities, are much higher. For example, data presented in Table VIII, p. 49, of Stoker et al. 1981, suggest an existing inventory in the Acid-Pueblo Canyon system of about 600 mCi, with an uncertainty (expressed as $\pm 2\sigma$) suggesting a range of 300-900 mCi. If 300-900 mCi are in the canyon system at the present time, then more than 150 mCi of activity must have been introduced as effluent between 1943 and 1951. Therefore, to reflect this uncertainty in the subsequent plutonium-routing calculations, we assumed a range of 150-3000 mCi as the initial input or effluent discharge to Acid Canyon for the period 1943-1950.

The data shown in Table XVI summarize the plutonium effluent discharges into two ephemeral stream channels at Los Alamos. The problem here is to describe the subsequent contaminant redistribution and transport by streamflow. Previous studies of contaminant transport in these stream channels suggest that most of the plutonium transport is associated with transported sediment (Stoker et al. 1981, p. 141). Therefore, to compute contaminant transport rates, we first had to compute runoff rates, then sediment transport rates and yields. The general procedure was to relate plutonium transport rates to sediment transport rates; the piecewise approximating hydrograph was used to relate plutonium yields to sediment yields for individual runoff events. Next, we summed yields from the individual storm events to estimate annual sediment and plutonium yields. These computations were made for the time periods shown in Table XVI. The result was a mass-balance calculation for each channel reach used to describe the drainage network from the upland areas to the confluence of Los Alamos Canyon with the Rio Grande.

To describe the contaminant yield calculations, we first needed to describe the hydrologic and sediment yield models as applied to the Los Alamos watersheds. This required characterizing the watersheds, estimating parameters, and conducting the model evaluation as described in Tables XIV and XV.

B. Application of the Models and Preliminary Evaluations

Drainage areas and the main channel network for Los Alamos Canyon (a principal drainage on the Pajarito Plateau, and the major emphasis of this analysis) are shown in Fig. 8. The upper 65.3-km^2 (25.5-mi.^{2}) drainage area of Los Alamos Canyon to the confluence of Guaje Canyon was subdivided into drainage areas and channel segments, as shown in Fig. 8, and as detailed in Table XVII. The land-use cover data in Table XVII correspond with the three vegetation types discussed above, except that the urban areas are listed without regard to vegetation type. The composite curve numbers reflect variations in soils, vegetation, and land use in that the distributed runoff simulation model was used to compute runoff from the 2-yr, 1-h storm using runoff curve numbers from 18 upland and lateral flow areas, as shown in Fig. 8. These distributed curve numbers varied from a low of 68 on the upland forest areas to a high of 85 from areas that were partially urbanized. The composite curve numbers also reflect the influence of transmission losses. For example, the composite curve number for channel segment number 8 was 77, without considering transmission losses, and 75 when transmission losses were included.

Additional features of the Los Alamos watersheds are summarized in Table XVIII. Drainage units labeled LA-1 through LA-5 refer to Los Alamos Canyon; AP-1 and AP-2 refer to Acid-Pueblo Canyon, G-1 refers to Guaje Canyon, and B-1 and B-2 refer to Bayo Canyon (see Fig. 8 and Table XVII). Hydrologic data for G-1 were estimated, based on runoff-drainage area relationships from watersheds LA-1 through LA-4, AP-1 and AP-2, and B-1 and B-2. Hydrologic data from LA-4 and G-1 were combined and routed to the Rio Grande to estimate runoff for the entire watershed designated LA-5 in Table XVIII. The 1-h rainfall depths (Table XIII) were adjusted following procedures outlined in Miller et al. (1973) to compute 1-h rainfall depths (87.5% of the point values) over the upper 25.2-mi.^{2} drainage area of Los Alamos Canyon. These rainfall depths were used to compute flood frequency data for the eight subwatersheds. Peak discharge values for the 2-yr flood are shown in Table XVIII.

Table XVII. Characteristics of the Los Alamos Canyon Watershed Above the Confluence with Guaje Canyon

Channel Segment	Drainage Area[a] (mi.^{2})	Drainage Area[a] (km^2)	Land-Use Cover (%)[b] Ponderosa Pine	Piñon Juniper	Urban	Composite CN[c]
1	9.1	23.6	90	--	10	76
2	10.6	27.5	80	10	10	75
3	5.8	15.0	60	--	40	77
4	8.2	21.2	50	20	30	75
5	20.7	53.6	60	20	20	75
6	1.9	4.9	70	10	20	76
7	3.9	10.1	30	60	10	75
8	25.2	65.3	50	30	20	75

[a]Total drainage area contributing above the downstream end of the channel segment.
[b]Approximate percentages of drainage areas with mixed forest cover dominated by ponderosa pine, woodland areas dominated by pinõn-juniper, and urban areas regardless of vegetation type.
[c]Composite curve number for the entire drainage area to match runoff volumes computed with distributed curve numbers and the 2-yr, 1-h rainfall. Includes the influence of transmission losses in the ephemeral stream channels.

Table XVIII. Selected Physical Features of Drainage Areas and Channel Segments in the Los Alamos Watershed
(English units used in this table correspond with units used in the simulation models)

Drainage Unit	Drainage Area (acres)	Mean Annual Flood Peak[a] (cfs)	Channel Segment at Watershed Outlet						Bed Material[c]	
			No.	Reach Length (mi)	Average Width[b] (ft)	Effective Hydraulic Conductivity (in./h)	Width (ft)	Slope	Manning n	Proportion of Silt-Clay	Median Particle Size (mm)
LA-1	5 807	72	1	4.10	4.4	2.00	10	0.018	0.040	0.066	0.62
LA-2	6 791	61	2	2.85	4.9	2.00	12	0.019	0.040	0.035	0.78
LA-3	13 253	101	5	2.20	15.2	2.00	19	0.024	0.035	0.026	0.42
LA-4	16 127	100	8	0.90	24.0	2.00	45	0.017	0.030	0.037	0.73
LA-5	37 293	180[d]	10	--	--	--	55	0.019	0.030	0.035	1.00
AP-1	3 696	68	3	3.30	14.6	0.50	14	0.019	0.040	0.026	0.80
AP-2	5 222	51	4	4.10	15.5	1.00	20	0.023	0.035	0.032	0.75
B-1	1 209	21	6	3.70	5.0	1.00	12	0.030	0.045	0.018	1.04
B-2	2 496	19	7	3.80	12.0	1.50	15	0.034	0.035	0.023	0.84
G-1	20 650	117[d]	9	--	--	--	43	0.027	0.035	0.075	0.57

[a]Calculated using the hydrologic model and the 2-yr, 1-h rainfall depth averaged over the 25.2-mi.^{2} drainage area.
[b]Average width over the entire channel reach as used in the transmission loss equation.
[c]Based on particle size analysis of channel bed material samples taken during periods of no flow.
[d]Calculated using peak discharge-drainage area relationships extrapolated from the simulated flood peaks on the eight subwatersheds comprising drainage area LA-4.

Procedures outlined in Table XIV were used to compare simulated flood peaks with measured flood peaks in the region (Dalrymple, 1965), as shown in Fig. 9. The curve labeled "upper" in Fig. 9 refers to the subwatershed with the highest peak discharge per unit area, and the curve labeled "lower" refers to simulated flood frequencies from the subwatershed with the lowest peak discharge per unit area. The upper and lower curves approximate envelope curves for the observed data shown in Fig. 9.

Simulated runoff data for the eight watersheds are shown in Table XVII, and exponents for the 2-yr flood were $C_4 = -0.13$ and $C_7 = -0.32$, which are within the probable ranges shown in Table XV. Therefore, based on the flood frequency analysis summarized in Fig. 9 and the values of C_4 and C_7 given above, the hydrologic model appears to be producing reasonable results.

Analysis of sediment concentration vs discharge rate produced an exponent of $C_9 = 0.27$ for the 2-yr flood on watershed LA-1. This value of $C_9 = 0.27$ is within the probable range shown in Table XV. Observed and computed suspended sediment discharge rates are shown in Fig. 10. The observed data represent sediment discharge rates computed from suspended sediment samples and estimated

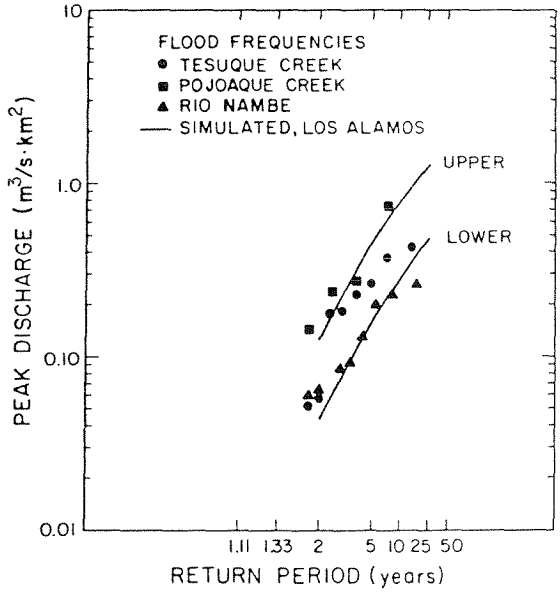

Fig. 9. Simulated and observed flood frequency data for Los Alamos watersheds and drainage areas within the region of Los Alamos, New Mexico.

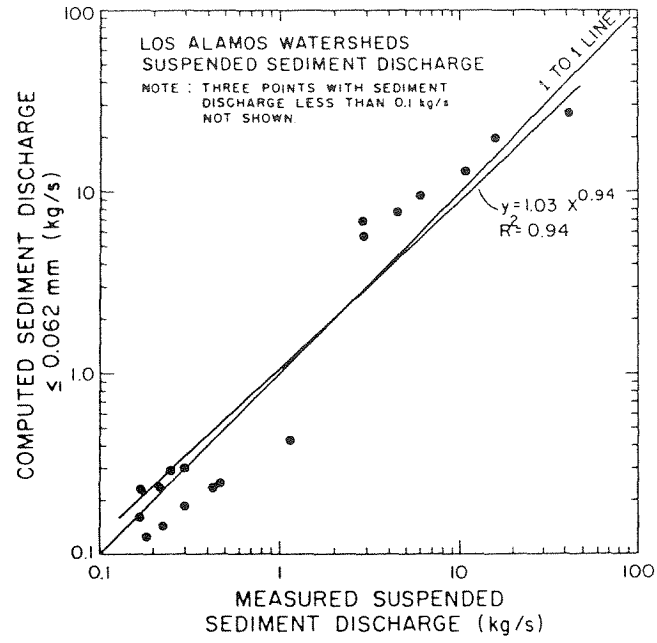

Fig. 10. Measured and computed suspended sediment discharge rates for seven channel sections in the Los Alamos Canyon watershed.

discharge rates. The data represent seven observations from watershed LA-1, two each from watersheds LA-2, LA-3, LA-4, and AP-2, one from LA-5, and five observations from Mortandad Canyon. Computed sediment discharge rates, shown in Fig. 10, were computed using the suspended sediment-transport capacity equation [Eq. (61)], the channel data shown in Table XVIII, and the given discharge rates. From these analyses, we concluded that the sediment discharge calculations were producing reasonable results for suspended sediment discharge rates. Finally, for the eight watersheds listed in Table XVII, we computed sediment yield for the 2-yr flood and related sediment yield to drainage area, as suggested in Table XV. The exponent was $C_{11} = 0.16$, which is outside the probable range (−0.50 to 0.0) shown in Table XV. Analysis of the channel features (see Table XVIII) suggested that channel width increased downstream, and Manning's n decreased downstream. However, channel slope and particle size characteristics varied more than they had previously. These factors, taken together, resulted in complex patterns of transport capacity and thus sediment yield with increasing drainage area. As a result, even though the derived value of $C_{11} = 0.16$ was outside the probable range,

we judged the sediment yield-drainage area relationship to be reasonable for this particular application at Los Alamos.

Plutonium discharge data (in nanocuries per second) were available for 14 of the 21 observations shown in Fig. 10. Based on plutonium concentrations in the channel alluvium and in the suspended sediment samples, the observed enrichment ratios varied from 1.4 to 13.3, with a mean of 5.5. The corresponding computed enrichment ratios, based on concentration in the channel alluvium and computed concentration with the suspended sediment, ranged from 2.9 to 7.0, with a mean of 5.2. Although the computed enrichment ratios had a smaller range, the mean was close to the observed mean. Based on total load calculations, including the estimated bed load, the computed enrichment ratios varied from 1.3 to 4.7, with a mean of 2.7. Observed enrichment ratios did not include bed-load sediment. Measured and computed plutonium flux values with suspended sediment are shown in Fig. 11.

A preliminary model evaluation was conducted using the criteria outlined in Tables XIV and XV. With one exception (C_{11} in the sediment yield-drainage area relationship), derived relationships had exponents within the probable ranges specified in Table XV. Moreover, flood frequencies computed with the hydrologic model agree with observed regional values. Computed sediment and plutonium discharge rates agreed with measured values, and mean computed enrichment ratios were within the probable range specified in Table XV. From these analyses, we concluded that the simulation models were producing reasonable results for runoff, sediment concentration and yield, and contaminant concentration and yield.

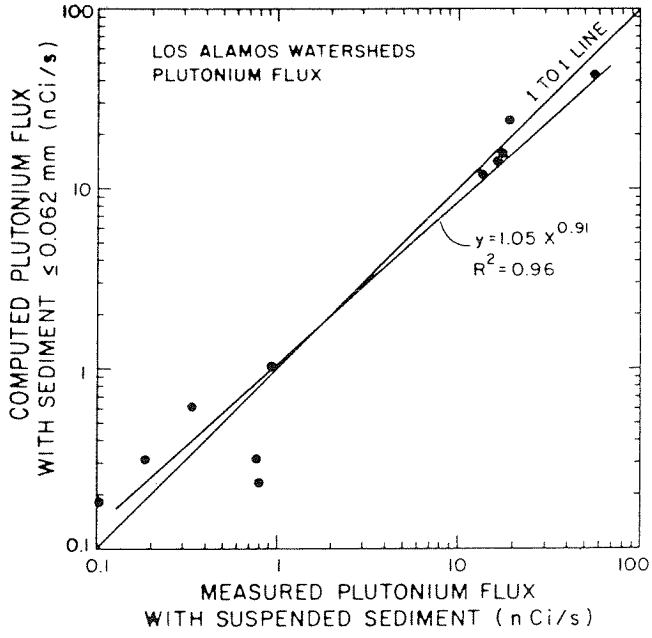

Fig. 11. Measured and computed plutonium discharge rates for five channel sections in the Los Alamos Canyon watershed.

C. Simulation of Annual Values and Projections

Based on procedures outlined in NOAA Atlas-2 (Miller et al. 1973), daily rainfall records at a point in Los Alamos were used to estimate maximum 1-h rainfall averaged over the drainage area. The approximating equation, in inches, is

$$P_1 = 0.039 + 0.553P_{24} \quad , \tag{67}$$

where P_{24} is the daily rainfall at a point, and P_1 is the maximum 1-h rainfall averaged over the drainage area. Equation (67) was applied to all daily rainfall data from 1943 to 1980. The 1-h rainfall data were then used as input to the hydrologic, sediment yield, and contaminant yield models for the watersheds shown in Tables XVII and XVIII. Individual storm values were summed to compute annual sediment yields. Observed data were then used to calibrate a series of regression equations relating snowmelt runoff to average March-April water content of the Jemez Mountains snowpack. The sediment transport model was then applied to these runoff data to derive regression equations relating average March-April water content of the snowpack to sediment yield for positions in the channels of Los Alamos Canyon. Snowmelt runoff in most other canyons is usually zero or insignificant and was omitted from the analysis.

Annual sediment yield (from storm runoff and snowmelt runoff) was then used in a discrete form of Eq. (66) to compute an annual mass balance for plutonium. Plutonium was discharged into Channel 1 (LA-1) and Channel 3 (AP-1). The plutonium outflow from these channel reaches was then taken as input to downstream reaches (Fig. 8), and the calculations were made for each channel segment until the confluence with the Rio Grande. Therefore, for each year (1943-1980), the calculations included input, output, and residual storage for each channel

segment or reach; by summation, the entire channel network was calculated.

Inventory estimates in the past (Stoker et al. 1981, and Nyhan et al. 1980) included significant plutonium amounts in inactive channel areas, in channel banks, and in overbank and flood plain areas. Hereafter, we refer to these areas as out-of-bank areas. Therefore, we say that a channel segment consists of the active channel and the out-of-bank areas. For computational purposes, we assume a rectangular cross section for the active channel and then a trapezoidal cross section for out-of-bank flow. When the discharge increases beyond the capacity of the active channel, the flow width increases with increasing discharge, according to the lateral slope of the out-of-bank areas. Flow in these out-of-bank areas can deposit sediment and associated contaminants if the existing sediment load from the active channel exceeds the transport flow capacity in the out-of-bank areas. Shallow flow depths and increased hydraulic resistance can reduce flow velocity, and thus transport capacity, in out-of-bank areas. However, the relationship between available sediment supply and out-of-bank transport capacity is a dynamic function of discharge rates, as well as being a function of the hydraulic roughness characteristics in out-of-bank areas. Under other circumstances, flow conditions in out-of-bank areas may produce sediment transport capacities in excess of the available sediment supply, which would suggest scour or erosion in out-of-bank areas.

Because runoff rates change with time at a given channel cross section, sediment deposition may occur at one time but erosion may occur at other times. For a given flow rate along a channel segment, deposition may be occurring at one position while, at the same time, erosion may be occurring at another position. Out-of-bank flow hydraulics and sediment transport mechanics are very complex in time and in space. However, we may compute estimates of lower and upper bounds for sediment transport capacity in out-of-bank areas during runoff events. If this is done for upstream and downstream cross sections on a given channel reach, then we can approximate limits for sediment deposition or out-of-bank erosion. A channel segment's net deposition or erosion is predicted to fall within these bounds.

The lower limit on transport capacity can be calculated by Einstein's procedure for computing the sediment trap efficiency of a settling basin developed in 1965 (see Borland 1971, for a useful summary). This procedure assumes deposition is occurring throughout the channel reach, so it sets a lower limit on transport capacity. If $t_{1/2}$ is the half-life for deposition to reduce sediment concentration by one-half, then the flow length, L, over which one-half the particles are deposited is

$$L = vt_{1/2} \quad , \tag{68}$$

where v is the mean velocity for the out-of-bank flow. The sediment fraction deposited over a distance x is

$$p = 1 - \exp(-0.693x/L) \quad . \tag{69}$$

Equations (68) and (69) can be applied if we have estimates for the velocity v and the half-life time $t_{1/2}$. This time can be estimated by

$$t_{1/2} = 0.657\, y/v_s n \quad , \tag{70}$$

where y is the average water depth in the out-of-bank areas, v_s is the particle fall velocity, and n is a parameter assumed to be 1.0 for rivers. Given a sediment supply (expressed as the concentration of suspended sediment delivered to the out-of-bank areas from overflow out of the active channel) at the upstream boundary of a channel reach, Eq. (69) is used to compute sediment transport capacity and deposition rates as functions of distance along the channel reach. Therefore, we now have estimated the lower bound for transport capacity and, from this, an upper bound for sediment deposition rate. Equation (66) also can now be applied to the out-of-bank areas to compute a potential maximum deposition rate for contaminants in out-of-bank areas. In this case, M and Q_s would refer to inventory and sediment yield in out-of-bank areas.

An upper limit on transport capacity in out-of-bank areas can be computed by applying the sediment transport equations used in the active channel. In this case, the procedure will be exactly the same as used in the active channel (and as described earlier), except that we assume a trapezoidal cross-sectional geometry for out-of-bank flow. If the computed transport capacity in out-of-bank areas exceeds the sediment supply from the active channel, then scour or erosion is predicted to occur. If the computed transport capacity is less than the sediment supply, then deposition is assumed to occur. In most cases, the deposition amount or scour is only a small fraction

of the total sediment yield for a runoff event. The estimated amounts were usually less than a few per cent, with the largest estimate being 15% deposition during one year in lower Pueblo Canyon.

1. Physical Features of the Channels and Out-of-Bank Areas. Basing our estimates on the annual floods computed for the period 1943-1980, we calculated the width of out-of-bank flows for the various channel reaches. Using the channel segments as defined in Table XVIII, we show the physical features of the active channels in Table XIX. Columns 7 and 8 in Table XIX show the estimated peak discharge of the 2-yr flood and the discharge capacity of the active channel. We estimate a small amount of out-of-bank flow for the 2-yr flood in the upper reaches (LA-1, LA-2, and AP-1), but note that the 2-yr flood is entirely within the active channel in the lower channel reaches.

Physical characteristics of the out-of-bank areas are summarized in Table XX. The average width of out-of-bank flow is shown in the third column of Table XX. These width estimates should be compared with the corresponding width estimates given in Stoker et al. (1981, Table VII, p. 49). The most significant difference is in the out-of-bank width (width of contaminated area) in mid Pueblo Canyon, AP-1. The value of 3.5 m, shown in Table XX, is about one-fourth the average width estimated by Stoker et al. (1981). The widths in Table XX were based on computed widths of out-of-bank flow based on measured channel cross sections at general positions in each channel reach. The values presented by Stoker et al. (1981) were based on measurements of cross sections at several positions, and they included no hydraulic calculations. The magnitude of these differences indicates the uncertainty involved in estimating average widths of out-of-bank flow events.

The out-of-bank flow events were the larger events, about 2 to 4 times the mean annual flood, suggesting more frequent runoff in the active channels than in the out-of-bank areas.

2. Calculation of Plutonium Concentrations and Inventories. Plutonium transport is assumed to be related to sediment yield

$$Q_{pu} = ER\, C\, Q_s \quad , \tag{71}$$

where Q_{pu} is plutonium yield in millicuries, C is the mean plutonium concentration in the alluvium in millicuries per ton, Q_s is the sediment yield in tons, and ER is the enrichment ratio. But from Eq. (66), we know that

$$Q_{pu} = k\, Q_s\, M \quad , \tag{72}$$

where k is a coefficient ($tons^{-1}$) and M is the currently available inventory in millicuries. Thus, k must be equal to (ER)(C)/M and, because C = M/S, where S is the mass of contaminated sediment,

$$k = ER/S \quad . \tag{73}$$

Values of k, for the individual channel reaches, are shown in the last column of Table XIX.

Equation (66) describes an entire channel reach. Let the subscript o refer to the out-of-bank areas. If we assume there is net deposition in the reach, then the discrete form of Eq. (66), with $\Delta t = 1$ year, becomes

$$M_i = M_{i-1} + I_i - kQ_{si}M_i \tag{74}$$

for the active channel, and

$$M_{oi} = M_{oi-1} + kQ_{soi}M \tag{75}$$

for out-of-bank areas where Q_s refers to the total sediment yield (deposition plus net yield), Q_{soi} refers to the out-of-bank deposition, M refers to the active channel inventory, and M_o refers to the out-of-bank inventory. Plutonium discharge at the end of the channel reach is then

$$Q_{pui} = kM_i(Q_{si} - Q_{soi}) \quad , \tag{76}$$

where $Q_{si} - Q_{soi}$ is the net sediment yield for the channel reach. Application of Eqs. (73)-(75) will give a lower bound for the net sediment and plutonium yield and an upper bound for the out-of-bank deposition of sediment and plutonium.

Calculations based on the above assumptions were made for the period 1943-1980, and the results are summarized in Tables XXI and XXII. The assumed initial input I (1943-1950 effluent discharge) to Acid-Pueblo Canyon was varied from 150 to 3000 mCi. The numbers shown in Tables XXI and XXII are all rounded to two decimal places. Accuracy to this many significant figures is not suggested, but significant digits are preserved to allow verification of the calculations. Also, notice that a 20-fold range in input results in a 6-fold range in the currently existing inventory. Finally, the listed values

Table XIX. Physical Characteristics of the Active Channels in the Los Alamos Watershed

Channel Reach	Length (m)	Average Width[a] (m)	Alluvium[b] Depth (m)	Surface Area (m^2)	Sediment Mass (mg)	Estimated 2-yr Flood (m^3/s)	Peak Discharge in Active Channel (m^3/s)	Coefficient k($Tons^{-1}$)
LA-1	6600	3.0	0.30	19 800	9 320	2.04	1.22	0.00113
LA-2	4600	3.7	0.30	17 000	8 010	1.73	1.22	0.00148
ACID	750	1.5	0.16	1 125	283	--	--	--
AP-1	5310	4.7	0.30	25 000	11 200	1.93	1.20	0.000906
AP-2	6600	5.2	0.30	34 300	16 200	1.44	2.15	0.000664
LA-4[c]	4990	9.8	0.30	48 900	23 000	2.83	3.99	0.000466
LA-5	2400	15.2	0.30	36 500	17 200	5.10	6.37	0.000622

[a]Average flow width to cover active channel bed along the channel reach.
[b]Assumed contamination depth in channel alluvium.
[c]Includes channel reaches LA-3 and LA-4 as defined in Table XVIII.

Table XX. Physical Characteristics of the Out-of-Bank Areas in the Los Alamos Watershed (includes the inactive channel and channel banks)

Channel Reach	Length (m)	Average Width[a] (m)	Alluvium Depth (m)	Surface Area (m^2)	Sediment Mass (mg)	Estimated Average[b] Peak Discharge (m^3/s)	Peak-Discharge Maximum[c] (m^3/s)
LA-1	6600	4.8	0.30	31 700	14 900	3.58	11.59
LA-2	4600	5.7	0.30	26 200	12 300	4.06	11.66
ACID	750	0.8	0.30	600	283	--	--
AP-1	5310	3.5	0.30	18 600	8 750	4.35	12.36
AP-2	6600	16.3	0.30	107 600	50 700	5.41	12.05
LA-4	4990	8.2	0.30	40 900	19 300	10.87	25.53
LA-5	2400	25.9	0.30	62 200	29 300	18.82	47.49

[a]Calculated maximum width (both sides of channel, but not including active channel) for largest out-of-bank flow event during period 1943-1980; average for the channel reach.
[b]Average peak discharge of out-of-bank flow events, 1943-1980.
[c]Maximum peak discharge for out-of-bank flow, 1943-1980.

Table XXI. Estimated Plutonium Inventory in Active Channels in the Los Alamos Watershed (a function of the assumed initial input I to Acid-Pueblo Canyon)

Channel Reach	Estimated Plutonium Inventory (mCi) as of 1980)				
	I = 150 mCi	I = 300 mCi	I = 750 mCi	I = 1500 mCi	I = 3000 mCi
LA-1	0.15	0.15	0.15	0.15	0.15
LA-2	0.23	0.23	0.23	0.23	0.23
ACID[a]	5.43	5.43	5.43	5.43	5.43
AP-1	3.16	4.43	8.22	14.61	27.34
AP-2	6.58	9.93	19.99	36.85	70.49
LA-4	4.70	5.50	7.86	11.83	19.76
LA-5	6.07	7.42	11.36	17.98	31.22
			Totals		
Acid-Pueblo	15.17	19.79	33.64	56.89	103.26
Upper LA	0.38	0.38	0.38	0.38	0.38
Lower LA	10.77	12.92	19.22	29.81	50.98
Total	26.32	33.09	53.24	87.08	154.62

[a]Value for Acid-Canyon averaged from estimates of Nyhan et al. (1982) and Stoker et al. (1981).

Table XXII. Estimated Plutonium Inventory in Out-of-Bank Areas in the Los Alamos Watershed (a function of the assumed initial input I to Acid-Pueblo Canyon)

Channel Reach	Estimated Plutonium Inventory (mCi) as of 1980				
	I = 150 mCi	I = 300 mCi	I = 750 mCi	I = 1500 mCi	I = 3000 mCi
LA-1	0.52	0.52	0.52	0.52	0.52
LA-2	0.34	0.34	0.34	0.34	0.34
ACID[a]	54.64	54.64	54.64	54.64	54.64
AP-1	4.13	7.75	18.74	36.67	72.83
AP-2	11.84	22.19	53.23	104.98	208.46
LA-4	3.30	5.95	13.72	26.75	52.80
LA-5	5.08	9.19	20.79	40.42	79.69
			Totals		
Acid-Pueblo	70.61	84.58	126.61	196.29	335.93
Upper LA	0.86	0.86	0.86	0.86	0.86
Lower LA	8.38	15.14	34.51	67.17	132.49
Total	79.85	100.58	161.98	264.32	469.28

[a]Value for Acid-Canyon averaged from estimates of Nyhan et al. (1982) and Stoker et al. (1981).

for Acid Canyon represent the average of corresponding estimated values derived using dimensions and concentration data presented by Nyhan et al. (1980) and Stoker et al. (1981), because Acid Canyon was excluded from the channel reaches analyzed herein.

Plutonium concentrations corresponding with the inventory estimates are shown in Tables XXIII and XXIV. Active channel concentrations are listed in Table XXIII, and the out-of-bank concentrations are listed in Table XXIV. Again, the data represent estimates corresponding with an assumed input range of I = 150 to 3000 mCi. Total plutonium concentration in the active channels is shown in Fig. 12. The vertical bars represent 95% confidence intervals about the mean concentrations from surveillance data. The curves shown in Fig. 12 connect the concentration estimates for each reach (data from

Table XXIII. Estimated Plutonium Concentrations per Unit Mass of Contaminated Sediments in the Active Channels of the Los Alamos Watershed (as of 1980)

Channel Reach	Estimated Plutonium Concentration (pCi/g)				
	I = 150 mCi	I = 300 mCi	I = 750 mCi	I = 1500 mCi	I = 3000 mCi
LA-1	0.02	0.02	0.02	0.02	0.02
LA-2	0.03	0.03	0.03	0.03	0.03
ACID	19.19	19.19	19.19	19.19	19.19
AP-1	0.27	0.38	0.70	1.24	2.32
AP-2	0.41	0.61	1.23	2.27	4.35
LA-4	0.20	0.24	0.34	0.51	0.86
LA-5	0.35	0.43	0.66	1.05	1.82

Table XXIV. Estimated Plutonium Concentrations per Unit Mass of Contaminated Sediments in the Out-of-Bank Areas of the Los Alamos Watersheds (as of 1980)

Channel Reach	Estimated Plutonium Concentrations (pCi/g)				
	I = 150 mCi	I = 300 mCi	I = 750 mCi	I = 1500 mCi	I = 3000 mCi
LA-1	0.03	0.03	0.03	0.03	0.03
LA-2	0.03	0.03	0.03	0.03	0.03
ACID	193.	193.	193.	193.	193.
AP-1	0.47	0.89	2.14	4.19	8.32
AP-2	0.23	0.44	1.05	2.07	4.11
LA-4	0.17	0.31	0.71	1.39	2.74
LA-5	0.17	0.13	0.71	1.38	2.72

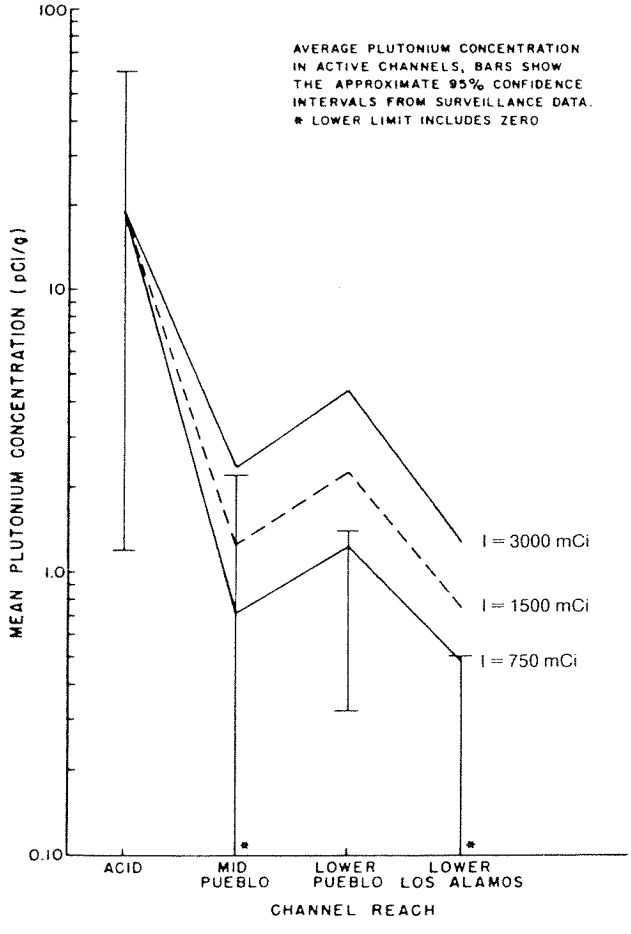

Fig. 12. Simulated and measured total plutonium concentration in active channels at Los Alamos.

Table XXIII, where reaches LA-4 and LA-5 are combined as lower Los Alamos). From these data, an initial input estimate of I = 750 mCi seems to fit the measured concentration data in the active channels better than larger values of I. Total plutonium concentrations in the out-of-bank areas are shown in Fig. 13. Again, the vertical bars represent measured data, and the curves connect the simulated data. For the out-of-bank areas, the initial estimate of I = 1500 mCi fits the measured data better than the other estimates. Total plutonium inventory is shown in Fig. 14. Again, the vertical bars represent confidence intervals about the means, suggested by surveillance data, and the curves connect estimates from the simulation model. In this case, an estimate for the initial input of I = 3000 mCi appears to be best in all reaches except lower Los Alamos Canyon. Finally, the data shown in Fig. 14 are also summarized in Table XXV.

Using the model and computational logic outlined earlier in this report, the simulation data summarized in Figs. 12-14 suggest that the initial input to Acid-Pueblo Canyon (effluent discharges from 1943-1950) was in the range of 750 to 3000 mCi. When the data in Table XXV are examined, a value of I = 560 mCi results for a total active channel inventory of about 45 mCi, which was also suggested by surveillance data. A value of I = 3100 mCi would result in a total inventory estimate of about 649 mCi, inferred from the surveillance data. However, Stoker et al. 1981, Table E-IV, suggest a 95% confidence interval for the total inventory of 631 ± 298 mCi ranging from 333 to 929 mCi. A corresponding range of initial input I is suggested

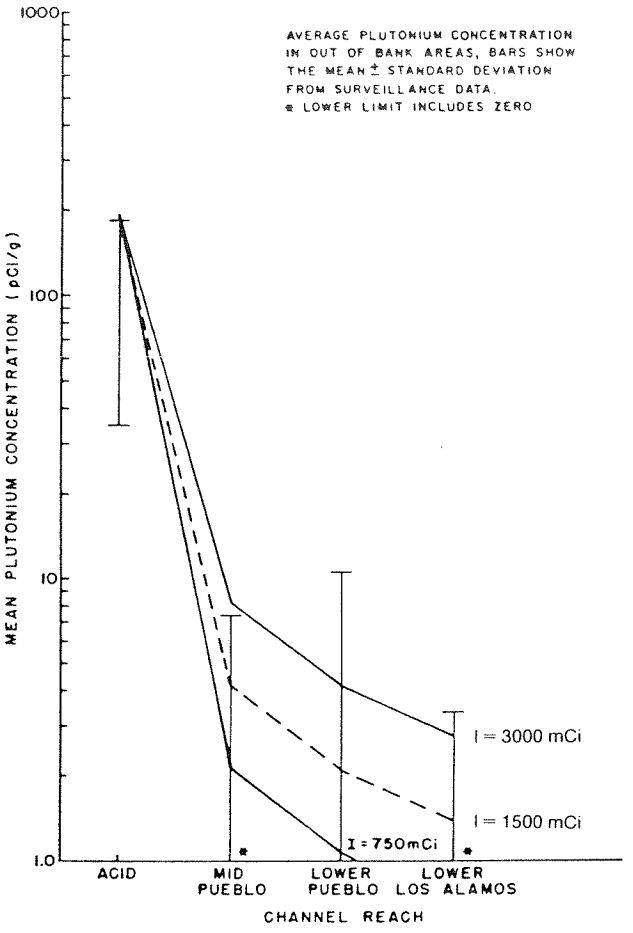

Fig. 13. Simulated and measured total plutonium concentration in out-of-bank areas at Los Alamos.

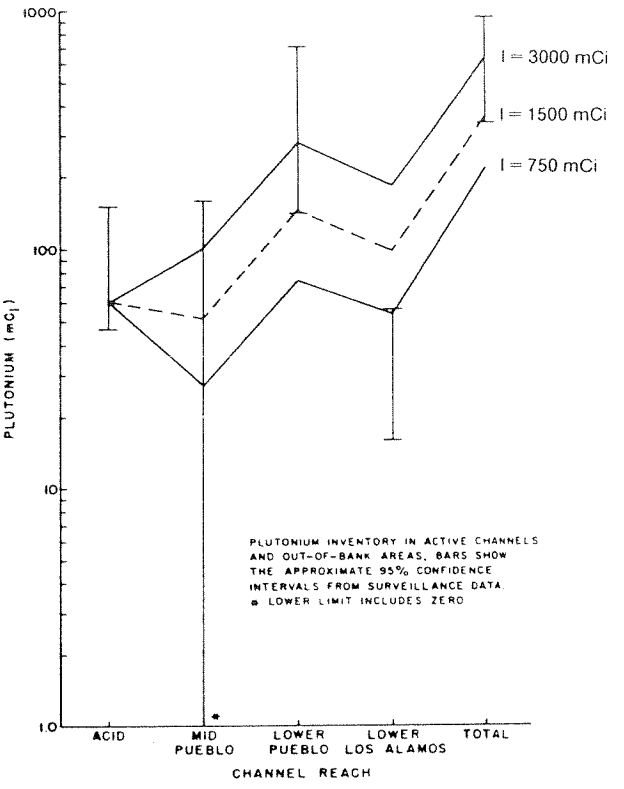

Fig. 14. Simulated and measured total plutonium inventory for stream channels at Los Alamos.

ranging from 1400 to 4700 mCi. Therefore, total inventory estimates, based on surveillance data, vary by a factor of 3 and the assumed initial input I varies correspondingly for the simulation model to produce inventory estimates varying by a factor of 3. Finally, because of differences in estimates of the out-of-bank width in Pueblo Canyon, the simulation model suggests less out-of-bank contamination than is suggested by the surveillance data. Under these conditions, even if the simulated and measured concentrations are comparable (see curves labeled I = 750 and 1500 in Figs. 12-14), the simulated total inventory is less than suggested by the surveillance data (Fig. 14). Therefore, when we are estimating plutonium concentration, a reasonable value for I probably ranges from 750 to 1500 mCi. When estimating total inventory, we would suggest a reasonable input value to be from 1500 to 3000 mCi. Therefore, the initial input is uncertain, but surveillance data suggest some rather broad ranges, as discussed above.

3. Projected Concentrations in the Active Channels. Earlier, we used historical rainfall data to estimate mean annual runoff and sediment yield from each channel segment. We assumed this mean annual sediment yield would be experienced during each year in the future, and we repeated the plutonium-routing and mass-balance calculations for the active channels. Figure 15 shows projected concentrations in mid Pueblo Canyon. Similar data for lower Pueblo and lower Los Alamos Canyons are shown in Figs. 16 and 17. Note that the projected concentrations vary by about a factor of 3, depending on the assumed value of the initial input I to Acid-Pueblo Canyon. Also, because we used mean annual sediment yields, the decay in mean

Table XXV. Summary of Plutonium Inventory Estimates from Surveillance Data and from the Simulation Model

Channel System	Surveillance Data (mCi)		Estimated Inventory (mCi) Using Simulator Model									
			I = 150 mCi		I = 300 mCi		I = 750 mCi		I = 1500 mCi		I = 3000 mCi	
	Active Channel	Out of Bank	Active Channel	Out of Bank	Active Channel	Out of Bank	Active Channel	Out of Bank	Active Channel	Out of Bank	Active Channel	Out of Bank
Acid	8.9	90.0	5.4	54.6	5.4	54.6	5.4	54.6	5.4	54.6	5.4	54.6
Pueblo	20.6	476.0	9.7	16.0	14.4	29.9	28.2	72.0	51.5	141.6	97.8	281.3
Acid-Pueblo	29.5	566.0	15.1	70.6	19.8	84.5	33.6	126.6	56.9	196.2	103.2	335.9
DP-Upper Los Alamos	4.4	2.2[b]	0.4	0.9	0.4	0.9	0.4	0.9	0.4	0.9	0.4	0.9
Lower Los Alamos	11.1	23.7	10.8	8.4	12.9	15.1	19.2	34.5	29.8	67.2	51.0	132.5
DP-Los Alamos	15.5	25.9	11.2	9.3	13.3	16.0	19.6	35.4	30.2	68.1	51.4	133.4
All channels	45.0	591.9	26.3	79.9	33.1	100.5	53.2	162.0	87.1	264.3	154.6	469.3

[a]From Stoker et al. (1981, Table VIII, p. 49), as modified to match the definition of channel reaches shown in Table XIX.
[b]Estimated inventory based on 20% of the original input remaining in the channel and 34% of that associated with bank sediments (Stoker et al., 1981, p. 193).

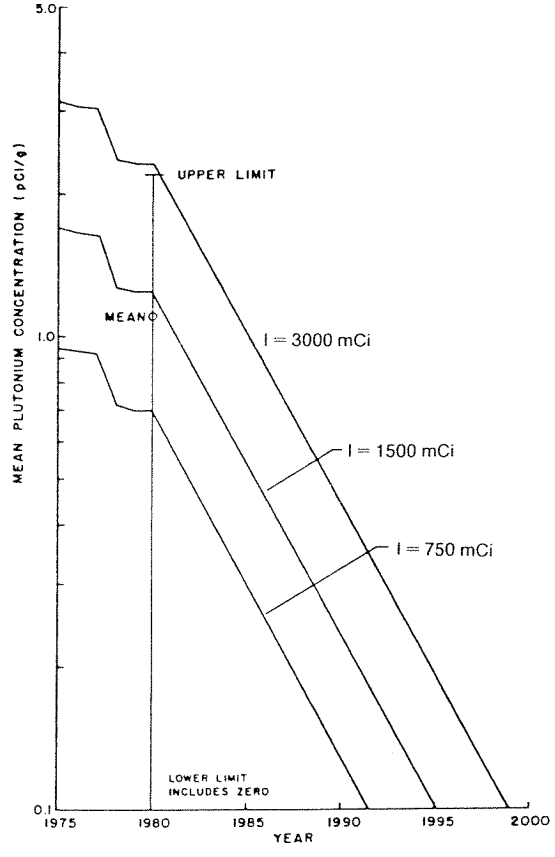

Fig. 15. Projected plutonium concentrations in the active channel in mid Pueblo Canyon. The circled point and bar show mean and 95% confidence interval from surveillance data.

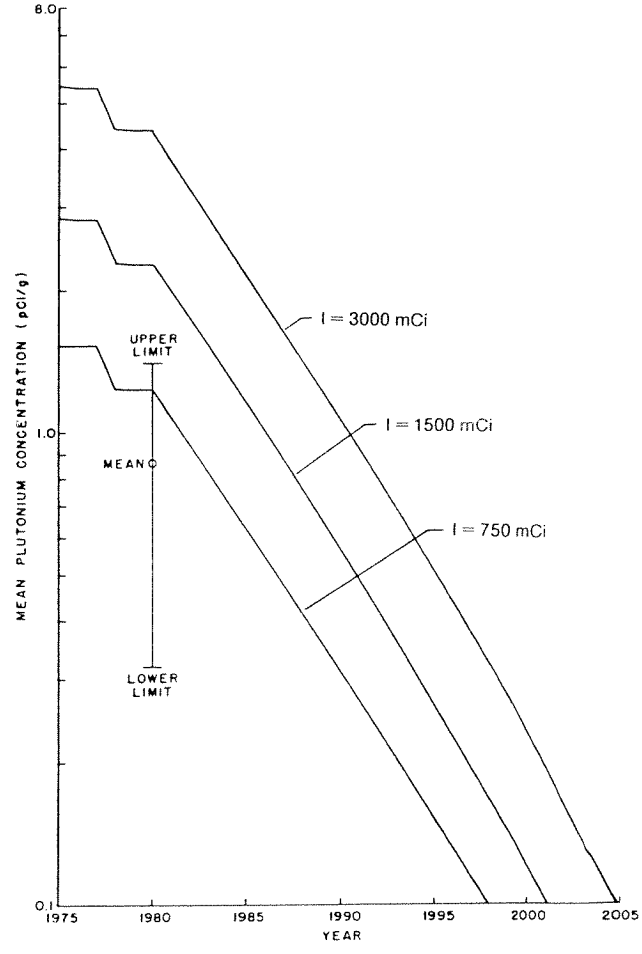

Fig. 16. Projected plutonium concentrations in the active channel in lower Pueblo Canyon. The circled point and bar show the mean and 95% confidence interval from surveillance data.

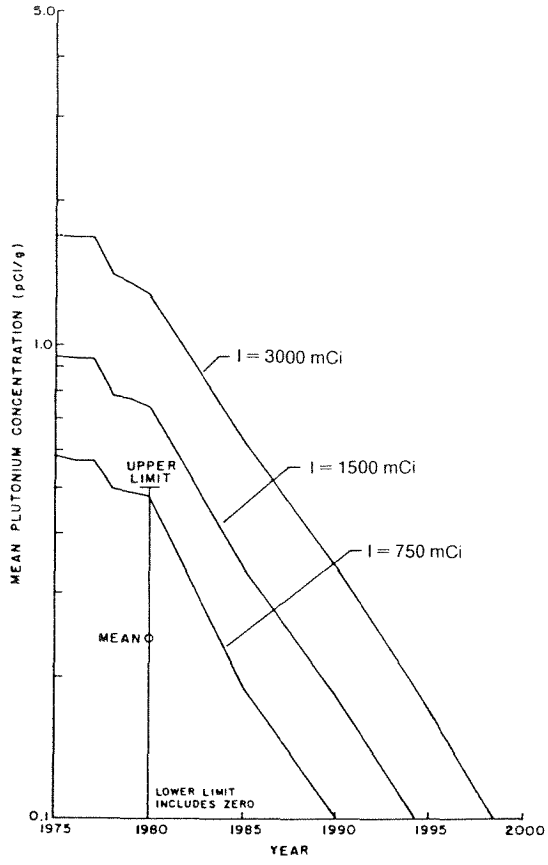

Fig. 17. Projected plutonium concentrations in the active channel in lower Los Alamos Canyon. The circled point and bar show the mean and 95% confidence interval from surveillance data.

concentration is very regular after 1980, but concentrations reflecting year-to-year variations in climatic input before 1980 varied much more than in the recent years. Therefore, these projections are highly uncertain. These uncertainties are due to approximations involved in the model formulations, errors in model parameters, and the obvious errors involved in assuming that the rainfall, runoff, and sediment yield, in the future, will exactly equal their average annual values over the last 38 years. Nonetheless, the projection data, summarized in Figs. 15-17, still estimate the future plutonium concentrations in active channel sediments. The data summarized in Figs. 15-17 include no out-of-bank areas or interacting active channels and out-of-bank areas. Out-of-bank hydraulics, erosion, and sediment transport processes are complex. Although we did not project out-of-bank processes on an average annual basis, we did estimate the active channel out-of-bank interaction for a large flood event occurring sometime in the future.

4. Projections for a Large Flood in Pueblo Canyon. A large flood, occurring within the entire Los Alamos watershed, might have sufficiently high discharge rates to erode or scour previously deposited sediment (and associated plutonium) from the out-of-bank areas and transport it out of the watershed. However, a large storm, limited to the Pueblo Canyon watershed, might result in erosion of out-of-bank areas in Pueblo Canyon and deposition in lower Los Alamos Canyon. This deposition might occur because transmission losses would tend to decrease the peak discharge (and thus sediment transport capacity) in the downstream direction. Because this deposited sediment could increase plutonium inventories in lower Los Alamos Canyon, we decided to analyze this situation as a "worst case."

Under the above assumption, net erosion is expected to occur in the active channel and out-of-bank areas in Pueblo Canyon, and net deposition is expected to occur in active channel and out-of-bank areas in lower Los Alamos Canyon. Therefore, we used the sediment transport equations [Eqs. (57) and (61)] for Pueblo Canyon and then the Einstein deposition model [Eqs. (68-70)] to compute deposition in the out-of-bank areas in lower Los Alamos Canyon, given no lateral inflow and the upstream input of water, sediment, and plutonium from Pueblo Canyon. The computations were made for a 50-yr flood in Pueblo Canyon.

If, as assumed, a 50-yr storm occurs over the Pueblo Canyon watershed, but not over the lower portion of the Los Alamos watershed, then runoff volume and peak discharge would decrease as the flood progressed through lower Los Alamos Canyon (channel reaches LA-4 and LA-5). Our calculations for runoff and sediment yield, under these assumptions, are summarized in Table XXVI. Notice that our calculations suggest a net erosion or scour in Pueblo Canyon and net deposition in active channels and out-of-bank areas in lower Los Alamos Canyon. Therefore, we predict a net reduction in plutonium inventory in Pueblo Canyon, and a net increase in lower Los Alamos Canyon. These relative changes for I = 1500 mCi are summarized in Fig. 18. The relative changes are much greater in

Table XXVI. Summary of Estimated Runoff and Sediment Yield for a 50-yr Flood in Pueblo Canyon

Channel Reach	Runoff Volume ($m^3 \times 10^3$)	Runoff Peak (m^3/s)	Net Sediment Yield (tonnes)	Sediment (in tonnes) Net Change in Reach: Active Channel Erosion	Active Channel Deposition	Out-of-Bank Erosion	Out-of-Bank Deposition
AP-1	94.3	21.1	1460	--	--	85	--
AP-2	104.2	21.8	3760	--	--	380	--
LA-4	86.6	14.4	2240	--	1520	--	69
LA-5	71.3	10.1	1660	--	580	--	13

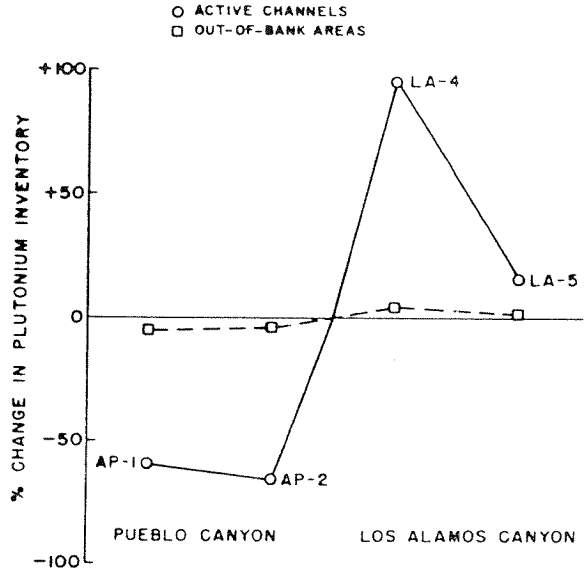

Fig. 18. Per cent change in plutonium inventory (or mean concentration) as the result of a 50-yr flood in Pueblo Canyon.

the more dynamic active channels than they are in the out-of-bank areas. Therefore, we predict that a major flood, of the type assumed in this analysis, might decrease the mean active channel and out-of-bank plutonium inventories some 60% and 4%, respectively. Deposition of sediment and associated plutonium in lower Los Alamos Canyon might increase the overall mean plutonium inventory in the active channel some 30% to 60% and, in the out-of-bank areas, some 1% to 2%. The lower increases in Los Alamos Canyon correspond with an assumed initial input of I = 750 mCi, and the higher ones, with an assumed I of 3000 mCi.

XI. SUMMARY AND DISCUSSION

A hydrologic model has been developed to simulate runoff rates and amounts occurring on semiarid watersheds, and procedures have been developed to estimate the model parameters from physical features of the watershed. The hydrologic model is an event model designed to simulate runoff that results from rainstorms. The model applied to watersheds at Los Alamos and, based on a regional flood frequency criterion, produced reasonable results.

Computing procedures developed for runoff hydrographs incorporate spatial variability owing to nonuniform runoff production and transmission losses. Basic concepts of open-channel flow hydraulics were used to develop a piecewise normal approximating hydrograph and to estimate the effective shear stress for sediment transport in alluvial channels with noncohesive sediments.

Sediment transport equations have been developed to compute sediment transport capacity according to the classes of sediment particle sizes. The approximating hydrograph and sediment transport equations are used to estimate sediment yield from semiarid watersheds with alluvial channels. Computed sediment transport rates were compared with observed rates from stream channels in Nebraska and New Mexico, and computed sediment yields were compared with observed yields from watersheds in Arizona. Although there were significant errors in computed sediment transport rates and yields for individual observations, the model

explained the trends in the observed data and produced reasonable estimates of sediment yield.

Procedures were developed to approximate the influence of particle sorting on enrichment of fine sediment particles and associated contaminants. Computed enrichment ratios for plutonium transport in stream channels at Los Alamos were comparable with measured enrichment ratios. As a result, computed plutonium transport rates explained the trends in observed transport rates in several channel reaches at Los Alamos.

Based on historical precipitation records at Los Alamos, procedures were developed to compute maximum 1-h rainfall, and thus runoff rates and amounts, from daily precipitation records. These estimated runoff data were then used to compute sediment yield for individual storm events from 1943 to 1980 on 10 subwatersheds draining into Los Alamos Canyon. These data provided plutonium transport rates in a mass-balance equation. The mass-balance equation was applied to compute plutonium outflow and storage in contaminated channel reaches at Los Alamos. Computed values of plutonium stored in the channel alluvium were roughly comparable with storage estimates based on plutonium concentration data obtained from alluvium samples collected for the environmental surveillance program. Based on the relative agreement between computed and estimated plutonium storage in the channel alluvium, mass-balance calculations were used to project plutonium storage and outflow to the year 2000. Although these projections are uncertain, they may help us design and interpret monitoring and remedial action programs.

Reasonably simple, yet physically based, simulation models have been developed to predict runoff, sediment transport and yield, and contaminant transport and yield from semiarid watersheds. Runoff and sediment transport provide the driving force and transport mechanisms for contaminant transport in alluvial stream channels. To the extent that runoff and sediment yield are predictable, contaminant transport and yield are predictable.

The procedures reported herein synthesize simplified procedures to describe and predict the complex processes of runoff, sediment yield, and contaminant yield from semiarid watersheds. At each point in the development, simplifications were made and simple relationships were used to approximate complex processes. There is considerable room to develop improved descriptions of the physical processes and improved models of the components describing them. Also, observed data, if available, can be used to improve parameter estimates for the simulation models. However, in the absence of improved models or observed data for improved parameter estimation, the procedures outlined in this report can be used for a first approximation of runoff, sediment yield, and contaminant yield from semiarid watersheds as described herein.

REFERENCES

Abeele, W. V., M. L. Wheeler, and B. W. Burton, "Geohydrology of Bandelier Tuff," Los Alamos National Laboratory report, LA-8762-MS (Oct. 1981).

Ardis, C. V., "A Storm Hydrograph Model for the Response and Variation of Small Rural Watersheds," Ph.D Thesis, University of Wisconsin (1972).

Ardis, C. V., "A Double Triangular Model for Generating Storm Hydrographs," Proc. 1st World Congress on Water Resources," Vol. 4, (1973), pp. 350-360.

American Society of Chemical Engineers, Task Force on Bed Forms in Alluvial Channels, John F. Kennedy, Chairman; "Nomenclature for Bed Forms in Alluvial Channels," Proc. Paper No. 4823, ASCE J., Hydraulics Division **92** (HY3), (1966).

Babcock, H. M. and E. M. Cushing, "Recharge to Ground Water from Floods in a Typical Desert Wash, Pinal County, Arizona," Trans. Am. Geophys. Union **23** (1) 49-56 (1941).

Bagnold, R. A., "The Flow of Cohesionless Grains in Fluids," Philos. Trans. R. Soc. London, Ser. A **246** (964), 235-297 (1956).

Bagnold, R. A., "An Approach to the Sediment Transport Problem from General Physics," US Geol. Surv. Prof. Paper 422-J (1966).

Barnes, H. H., "Roughness Characteristics of Natural Channels," US Geol. Surv. Water Supp. Paper 1849 (1967).

Borland, W. M., "Reservoir Sedimentation," Chapter 19 in River Mechanics, Vol. II (H. W. Shen, Ed. and Publisher, 1971).

Branson, F. A., G. F. Gifford, K. G. Renard, and R. F. Hadley, *Rangeland Hydrology*, 2nd ed., Society for Range Management, Denver, Colorado (Kendall/Hunt Publishing Co., Dubuque, Iowa, 1981).

Burkham, D. E., "A Method for Relating Infiltration Rates to Streamflow Rates in Perched Streams," US Geol. Surv. Prof. Paper 700-D, D266-D271 (1970a).

Burkham, D. E., "Depletion of Streamflow by Infiltration in the Main Channels of the Tucson Basin, Southeastern Arizona," US Geol. Surv. Water Supp. Paper 1939-B (1970b).

Chow, V. T., *Open-Channel Hydraulics* (McGraw-Hill Book Co., New York, 1959).

Colby, B. R. and C. H. Hembree, "Computation of Total Sediment Discharge Niobrara River near Cody, Nebraska," US Geol. Surv. Water Supp. Paper 1357 (1955).

Dalrymple, T., "Flood Peak Runoff and Associated Precipitation in Selected Drainage Basins in the United States," US Geol. Survey. Water Supp. Paper 1813 (1965).

Diskin, M. H. and L. J. Lane, "Application of a Double Triangle Unit Hydrograph to a Small Semiarid Watershed," *Hydrology and Water Resources in Arizona and the Southwest* 6, 125-135 (1976).

Einstein, H. A., "Formulas for the Transportation of Bed Load," ASCE J. 107, 561-597 (1942).

Einstein, H. A., "Bed-Load Transportation in Mountain Creek," US Dep. Agric., Soil Conservation Service document SCS-TP-55 (1944).

Einstein, H. A., "The Bed-Load Function for Sediment Transportation in Open Channel Flow," US Dep. Agric. Tech. Bull. 1026 (1950).

Environmental Surveillance Group (HSE-8), "Formerly Utilized MED/AEC Sites Remedial Action Program. Radiological Survey of the Site of a Former Radioactive Liquid Waste Treatment Plant (TA-45) and the Effluent Receiving Areas of Acid, Pueblo, and Los Alamos Canyons, Los Alamos, NM," U.S. Dep. of Energy, DOE/EV-0005/30, LA-8890-ENV (1981).

Foster, G. R., L. J. Lane, J. D. Nowlin, J. M. Laflen, and R. M. Young, "Estimating Erosion and Sediment Yield on Field-Sized Areas," Trans. Am. Soc. Agric. Eng. 24 (5), 1253-1262 (1981).

Graf, W. H., *Hydraulics of Sediment Transport* (McGraw-Hill Book Co., New York, 1971).

Jordan, P. R., "Streamflow Transmission Losses in Western Kansas," ASCE J., Hydraulics Division 103 (HY8), 905-919 (1977).

Knisel, W. G., Ed., "CREAMS: A Field-Scale Model for Chemicals, Runoff, and Erosion from Agricultural Management Systems," US Dep. Agric., Conservation Research report 26 (1980).

Kraatz, D. B., "Irrigation and Canal Lining," (Rome, United Nations Food and Agriculture Organization, 1977).

Lane, L. J., "A Proposed Model for Flood Routing in Abstracting Ephemeral Channels," *Proc. Hydrology and Water Resources in Arizona and the Southwest* (Ariz. Water Resource Association and Arizona Academy of Science, Prescott, Arizona, May 1972), Vol. 2, pp. 439-453 (1972).

Lane, L. J., "Transmission Losses," Chapter 19 in *National Engineering Handbook*, Sec. 4, Hydrology (US Dep. Agric., Soil Conservation Service, Washington, D.C., 1980).

Lane, L. J., "A Distributed Model for Small Semiarid Watersheds," ASCE J., Hydrology Division 108 (HY10), 1114-1131 (October 1982a).

Lane, L. J., "Development of a Procedure to Estimate Runoff and Sediment Transport in Ephemeral Streams," in Proc. Exeter Symp. Inter. Assoc. of Hydrological Sciences, Exeter, England, IAHS Pub. No. 137, pp. 275-282 (July 1982b).

Land, L. M., M. H. Diskin, and K. G. Renard, "Input-Output Relationships for an Ephemeral Stream Channel System," J. Hydro. 13, 22-40 (1971).

Lane, L. J., D. A. Woolhiser, and V. Yevjevich, "Influence of Simplifications in Watershed Geometry in Simulation of Surface Runoff," Colorado State University, Fort Collins, Colorado CSU Hydrology Paper No. 82 (1975).

Printed in the United States of America
Available from
National Technical Information Service
US Department of Commerce
5285 Port Royal Road
Springfield, VA 22161

Microfiche (A01)

Page Range	NTIS Price Code	Page Range	NTIS Price Code	Page Range	NTIS Price Code	Page Range	NTIS Price Code
001-025	A02	151-175	A08	301-325	A14	451-475	A20
026-050	A03	176-200	A09	326-350	A15	476-500	A21
051-075	A04	201-225	A10	351-375	A16	501-525	A22
076-100	A05	226-250	A11	376-400	A17	526-550	A23
101-125	A06	251-275	A12	401-425	A18	551-575	A24
126-150	A07	276-300	A13	426-450	A19	576-600	A25
						601-up*	A99

*Contact NTIS for a price quote.